

**Bulletin of the Seismological Society of America**  
**Studies of mechanism for water level changes induced by teleseismic waves**  
 --Manuscript Draft--

<b>Manuscript Number:</b>	BSSA-D-12-00360R2
<b>Article Type:</b>	Article
<b>Section/Category:</b>	Regular Issue
<b>Full Title:</b>	Studies of mechanism for water level changes induced by teleseismic waves
<b>Corresponding Author:</b>	Yan Zhang, Ph.D. Institute of Geology and Geophysics, Chinese Academy of Sciences Beijing, CHINA
<b>Corresponding Author's Institution:</b>	Institute of Geology and Geophysics, Chinese Academy of Sciences
<b>Corresponding Author E-Mail:</b>	eve_041744@163.com
<b>Order of Authors:</b>	Yan Zhang, Ph.D. Li-Yun Fu Fuqiong Huang Yuchuan Ma Lian-feng Zhao Bo Zhao
<b>Abstract:</b>	The 8.0 Wenchuan earthquake of May 12, 2008 induces large-amplitude water level changes at intermediate and far fields (epicentral distance >1.5 fault rupture length) in Chinese mainland. According to the seismograms, the co-seismic water level changes are attributed to the dynamic strain induced by the passage of seismic waves, most probably long period surface waves. Although many hydrologic changes induced by teleseismic waves have been reported, the mechanisms responsible for the changes still remain unclear. We invoke Skempton's coefficient B in this paper to explain those co-seismic water level changes documented in the intermediate and far fields. Some of those abrupt coseismic water level changes, for which the variation of the co-seismic water level, Skempton's coefficient B and the effective pressure preserve uniformity ( all increase or all decrease ) are found to favor the consolidation/dilatation induced by the shaking of teleseismic waves. While the other part of those coseismic water level changes, can be explained with the enhanced permeability caused by fracture clearing or overcoming the capillary entrapment in porous channels of the aquifer induced by the shaking of teleseismic waves, and most of those wells lie in basins or in hollows, where the formation is relatively stable and stiff.
<b>Author Comments:</b>	Although coseismic water level changes induced by teleseismic waves have been widely studied, the mechanism responsible for the changes are usually obscure. We invoke the Skempton's coefficient B and effective pressure in this paper to explore the mechanism.
<b>Suggested Reviewers:</b>	Chi-yuen Wang chiyuen@berkeley.edu He is an expert in the region we studied in this paper, and several of his papers have been the references of this manuscript.
<b>Opposed Reviewers:</b>	Yaowei Liu  he has a conflict with one of the author
<b>Response to Reviewers:</b>	I will include this information in files that will be uploaded.

**Reviewer #1:** The authors made some improvements on their manuscript based on reviewers' comments, but the revised manuscript still comes short on some important issues pointed out by this reviewer:

For example, the revised manuscript does not include any well logs as suggested by this reviewer. The authors refused this suggestion because (line 96) including the well logs "will possess so much space". But factual data must be included in scientific papers in order to support their reasoning. Without factual data, their statements such as 'aquifers in the basins are relative stiff' (lines 23, 66, 227, 390, 416) become pure speculation. Also, simplified geologic logs, as needed here, will not take too much space.

**Reply:** (Whether the "logs" mean the logging pictures? Since those wells are observation stations for the natural earthquakes, there are only "borehole columnar diagram", always those drilling wells have the loggings.) We have added those borehole columnar diagrams into "Figure 8-plus figure-borehole columnar diagram", which really possess so much space (we get those borehole columnar diagram from the <China earthquake monitoring records series> (which is written by different Subordinate units (earthquake administration of each provinces and different institutions) of China Earthquake Administration, and published in Beijing in different years by Seismological Press (in Chinese)), the pictures are designed already, some boreholes columnar diagrams explained in detail and some just in shot). Those information obtained from the borehole columnar diagrams together with the aquifer lithology have already been added into Table 1 during the last modification, but we have not clarified that clearly. Corresponding modifications in the paper are show in (Line: 105-108)

Please consider about whether to include all those diagrams in this paper finally, or just to see that to check the geology conditions.

The formation and aquifer of the basins are relatively more stable and stiff comes from the mechanical structure point, those vaulted/arched and concave structures are more stable and stiff than the flat ground. For example, the bridge always constructed to be vaulted, which will be more stable and stiff. We think this is reasonable and not a pure speculation. (See Line:236-242; Line:451-454 )

As another example, the revised manuscript does not include any seismograms as suggested by this reviewer. The authors argued that (line 397-400) the distance from the nearest seismic station is about 40 km, 'so the seismogram could not reflect the real characteristics of the geology'. This statement may be incorrect if the local geology of the seismic station is similar to that near the well. But the authors did not

provide any more detailed reason before they dismissed the reviewer's suggestion.

**Reply:** Because of the limitation of the objective observation settings, we can only get the seismograms of the 48 national stations (48 stations are show in the following picture). After comparison, generally we may use the seismograms of 4 national stations (stations in red circles in fig 1) to analyze the corresponding water level observations (stations in red circles in fig 2), which are near those national stations (the distances between the water level wells and the national seismogram stations are approximately less than 100km.)

As show in the two pictures, we use the seismogram of Sheng yang (SNY) national station to analyze Fuxin well (there are about 102.81 km between them), while Taiyuan (TIY) national station is corresponding to well e (there are about 40.903 km between them); Lanzhou (LZH) station is corresponding to well g (there are about 19.82 km between them); and Hefei (HEF) station is corresponding to well k (there are about 91.57 km between them), and the geology conditions are very similar (the main bed rock of Fuxin well and Shengyang station are both granite; Well e is in the east of Taiyuan basin, bed rock of well e and Taiyuan station are both limestone; Well k is in Chuhe river major dislocation and Hefei--Dongguan fracture intersection; bed rock of well g and Lanzhou station are both sandstone).

However, because the Z-component seismogram of TIY national station is deficient, we have to give up the analysis of Z component of the seismogram in TIY station. The waveforms in LZH station is also deficient, there may be some disturbances (Figure 7). There are only hourly water level data of Fuxin well (minute data observation strats from 2009), so we can not use that to do comparison with the seismogram. In general, we can only use well e and well k to do the comparisons between the water level changes and the seismograms.

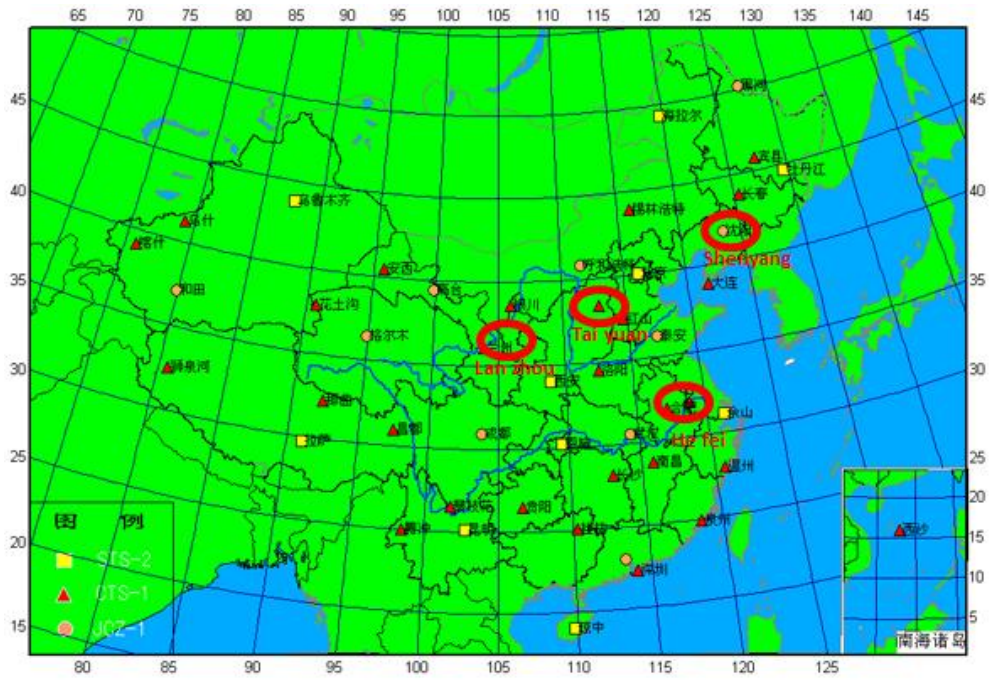


Fig 1. Distribution of national seismic stations in the Chinese mainland.

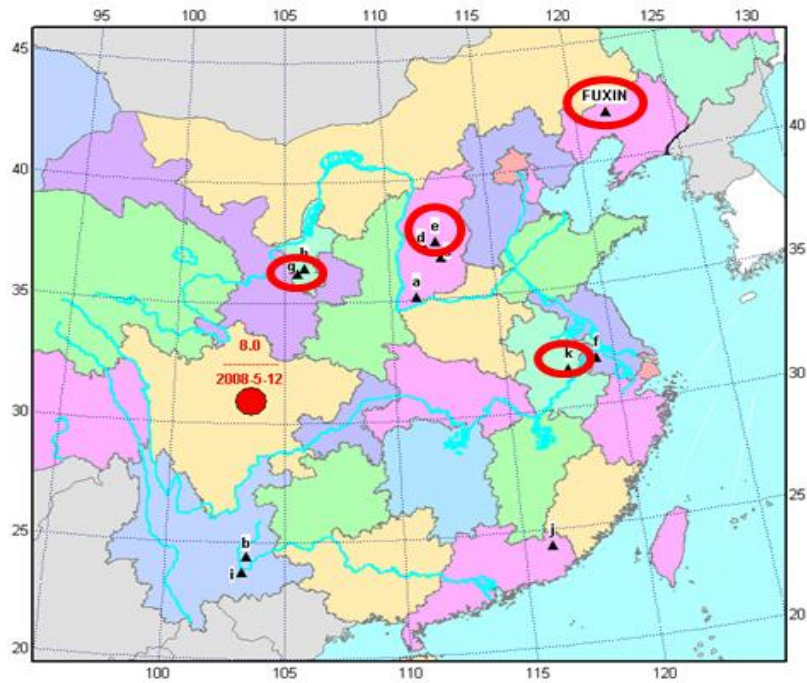
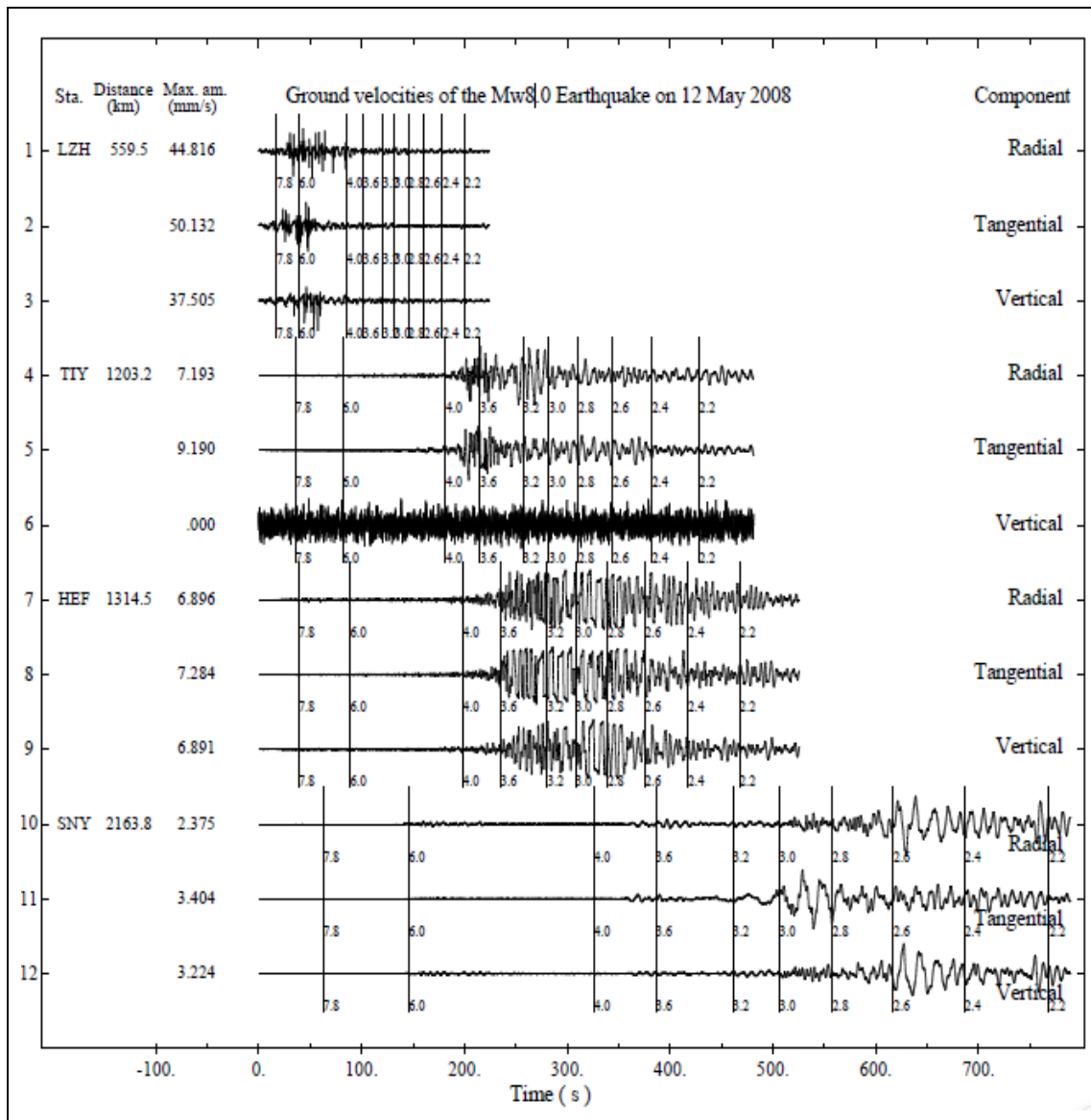


Fig 2. Stations used in this paper



**Figure 7.** Seismograms of the selected 4 national stations for the  $M_s$  8.0 Wenchuan earthquake. The stations are ordered according to their epicentral distances. The station names and maximum amplitudes are listed on the left-hand side and are measured in millimetres per second. Marks (vertical lines) on the waveforms indicate apparent group velocities. “0” is the time of Wenchuan earthquake: at 14:27:59.5, May12, 2008 (Chinese time). (This plotting pattern of seismograms are coined by [Zhao et al.\(2008\)](#)).

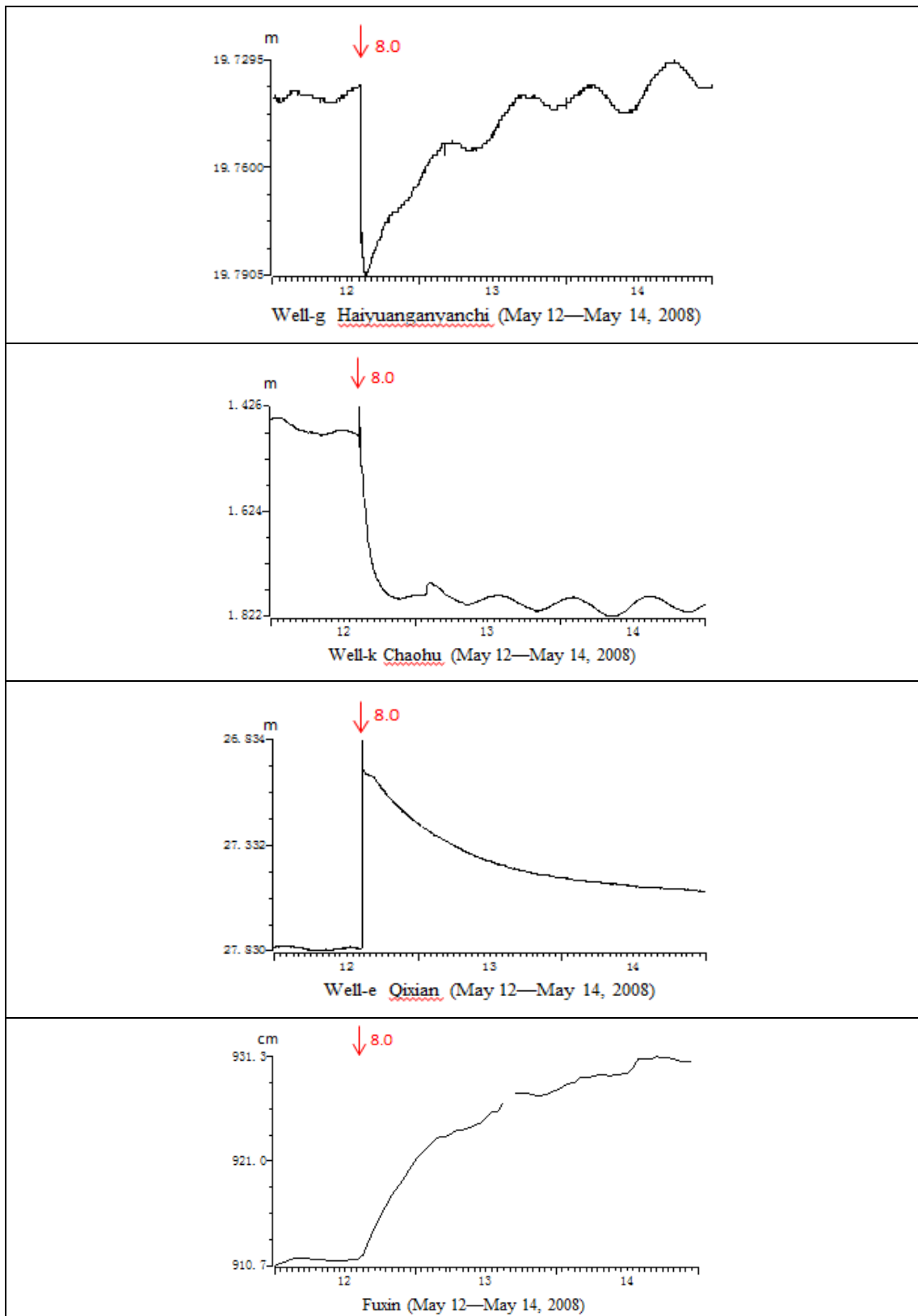


Fig 3: Co-seismic water level changes of the 4 wells.

Well(water level)/ Station(seismogram)	Occurrence time of water level change/min	Arrival time of surface wave/s	Seismogram quality
(g) Haiyuanganyanchi / LZH	14:27:00, May 12, 2008	14:28:24.5, May 12, 2008	deficient
(e) Qixian / TIY	14:35:00, May 12, 2008	14:30:59.5, May 12, 2008	(z component) deficient
(k) Chaohu / HEF	14:32:00, May 12, 2008	14:31:59.5, May 12, 2008	good
Fuxin (only hour data) / SNY	14:??, May 12, 2008	14:36:19.5, May 12, 2008	good

**Table 4.** Occurrence time of water level changes and arrival time of surface waves.

From the occurrence time of water level changes and the arrival time of surface waves of well e and well k (Table 4), we find the co-seismic water level changes are attributed to the passage of surface waves in the two wells. From that, we may infer: in other wells the co-seismic water level changes are attributed to the dynamic strain induced by the passage of teleseismic waves, most probably surface waves, which have relatively larger amplitude of oscillation, corresponding to relatively larger energy. The similar conclusion has been proposed by Sil and Jeffrey (2006), West *et al.* (2005) and Chadha *et al.* (2008).

Since well g and well k are all induced by the dilatations incurred by teleseismic waves, we can do some comparisons between them. From the seismograms we can see, the velocity amplitude of LZH (near well g) is much larger than that of HEF (near well k), so the energy of the teleseismic waves is much larger in well g than in well k (energy is in direct proportion to the square of the amplitude of oscillation). However, the amplitude of the co-seismic water level changes are not only related to the energy, but also connected with the different local geology conditions, such as the extent of the coupling between the solid matrix and the fluid (Skempton's coefficient  $B$  ( $B$  value of well k is larger than that of well g)), so the amplitude of the coseismic water level change of well k is larger than that of well g.

Because of the low temporal resolution of the water level data, further analysis of the steps could not be made. Co-seismic water level changes occurred in the 2 wells during the passage of surface waves. More precise estimation of the timing of the step could not be made because of the low temporal resolution of the water level data. Inevitably, there are difference of geographic position between the observation of seismograms and water levels, and there are also some errors on the manual amplitude reading, both of which could cause some influence on the analysis.

Figure (1) (2) (3) are not included in the paper, just show them to

the reviewer.

Corresponding modifications in the paper are show in (Line: 400–457)

The authors often make broad-brushed speculations that are devoid of observational or theoretical support. Examples include (line 231–233) “The spreading of shear waves may cause dilatation of the aquifer medium, which can broaden the porosities and give birth to new fractures, ?” The problem with this statement was pointed out by the other reviewer, but the authors did not take up the suggestion.

**Reply:** Yes, this is really not precise, and we have modified the “shear waves” into “teleseismic waves”. (Line: 244).

Also, as pointed out by this reviewer and shown in their Figure 1, the geology of the 12 wells in this paper is diverse and very complicated, which must have affected the response of the wells. Without consideration of such diversity and complexity, it may be hazardous to apply simple models such as poroelastic strain, consolidation-dilation, and increasing permeability.

**Reply :** The geology conditions are important, and complex, so we refer to the pre- and post- earthquake Skempton’ s coefficient  $B$  ( it is an important aquifer parameter, which reflect the extent of the coupling between the load and the fluid of the stiff rock matrix (Nur and Byerlee, 1971), it can reflect the local aquifer property), the inferred effective pressure change together with the co-seismic water level change to analyze the mechanism. And the mechanism analysis is reasonable.

As we have explained in the Appendix (Line: 657–659, 673–679) “ One thing needs to be clarified: We haven’ t applied the static equations directly to relate pore pressure changes to seismic waves. We use those static equations for the impact of the tidal strain on the aquifer medium before and after the Wenchuan earthquake, so as to obtain the pre- and post- earthquake Skempton’ s coefficient  $B$  (those two periods can be recognized as two independent quasi-static processes), so the poroelastic static equations can be applied” . We have not simply use the poro-elastic theory, while use it to calculate the pre- and post- earthquake  $B$  values. We use the variation of the co-seismic water level, Skempton’ s coefficient  $B$  and the effective pressure to judge the mechanism of those co-seismic water level changes. (“When the variation of the co-seismic water level, Skempton’s coefficient  $B$  and the effective pressure preserve uniformity ( all increase or all decrease, the water level changes are found to favor the consolidation/dilatation induced by the shaking of teleseismic waves. While the other part of those coseismic water level changes, can be explained with the enhanced permeability caused by fracture clearing or overcoming the capillary entrapment in



porous channels of the aquifer induced by the shaking of teleseismic waves.” )

Together with the seismograms of HEF (corresponding to well k) and TIY (corresponding to well e) stations (as suggested by the reviewer), we can infer “Dynamic strain induced by the passage of seismic waves, most probably long period surface waves might be the cause of water level changes in the far-field” The similar conclusion has been proposed by Sil and Jeffrey (2006), West et al. (2005), and Chadha et al. (2008).

In the discussion part, we analyze: according to the diverse and very complicated geology conditions, we may focus on 1—2 wells, to do much more deeply analysis in future, so as to reveal the mechanisms more clearly.

**Corresponding modifications in the paper are show in (Line: 399–456)**

The authors are also careless in citing their references. A clear example is (line 27–28): “ ? many (hydrologic responses) occurred at great distances from the ruptured fault where static stress changes are relatively small (? Liu and Manga, 2009 ?). But ‘Liu and Manga (2009)’ is a laboratory study with dynamic stresses; it is therefore inadequate as an reference for hydrologic responses occurring ‘at great distances’ with “static stress changes”.

**Reply:** This is really a careless problem, and we have checked those citations carefully this time, and as indicated by the reviewers, we should be much more careful and strict from now on. Thank you very much!

**We modified the Introduction, and please see those annotated green colors.**

The English of the manuscript is much to be desired. For example, the following sentence (line 421–423) is opaque to this reviewer: “From the analysis of Fuxin well, we can see a consolidation with large enough energy may also incur an enhanced permeability by overcoming the capillary entrapment in porous channels or by fracture clearing ?”

**Reply:** We have changed the sentence into “From the analysis of Fuxin well, we can see a consolidation with large enough energy may overcome the capillary entrapment in porous channels or clear the fractures, and incur an enhanced permeability.” (See Line: 474–476).

In summary, this paper is interesting mainly because of the new water-level data. The author may be able to strengthen their models by providing wells logs and some seismograms. To make their paper acceptable the authors should remove their broad-brushed speculations, make more careful use of references, and improve the English of the paper.

**Reply:** The reviewer is very careful and strict, those are the vital characters we need to improve in our future study.

**Reviewer #2:** The paper is much improved, only minor things remain:  
The paper should be grammatically corrected and simple sentences should be used.

e. g.

**Reply:** Thank you very much for pointing out those sentences need to be modified. We have changed those sentences and also checked the whole manuscript.

Page 7, Line 164..Depth of those wells are show in Table 1,.....

**Reply:** We have changed the sentence into “Depths of those wells analyzed in this paper are all less than 1km (Table 1).” see: Line 175.

Page 9 Line 191 after fullstop “Which” starts.....”value of B will increase/decrease. Which indicating shaking induced by the transmission of teleseismic waves may cause consolidation/dilatation of the aquifer

**Reply:** We have changed the sentence into “Hence, shaking induced by the transmission of teleseismic waves may cause consolidation/dilatation of the aquifer, and lead to the increase/decrease of the water level.” See: Line 203.

Page 10, Line 224...,.....”The local geological structure of each well is important (Table 1), We just find that most of those wells in which... the words like “We just find”..doesn’t make any sense.

There are more sentences which need to be rechecked and modified.

**Reply:** We have deleted “we just find.”

The sentence is changed into 2 sentences “The local geological structure of each well is important (Table 1), we find that most of those wells in which permeability increase induced by shaking of teleseismic waves, stay in basins or in hollows (well e, f, h, i and Fuxin). Due to the mechanical structure, the formation of the basin (or hollow) is relatively solid and stiff, and the deformation (consolidation or dilatation) will not easily to be incurred, then the energy of shaking may be inclined to induce the fracture clearing (unclogging) so as to increase permeability.” See: Line 235.

# Studies of mechanism for water level changes induced by teleseismic waves

Yan Zhang<sup>1</sup>, Li-Yun Fu<sup>1</sup>, Fuqiong Huang<sup>2</sup>, Yuchuan Ma<sup>2</sup>, Lian-feng Zhao<sup>1</sup>, and Bo Zhao<sup>2</sup>

1. Key Laboratory of the Earth's Deep Interior, Institute of Geology and Geophysics, Chinese Academy of Sciences, No. 19, Beitucheng Western Road, Beijing 100029, China. E-mail: eve\_041744@163.com; lfu@mail.iggcas.ac.cn
2. China Earthquake Networks Center, No. 5, Sanlihenanmeng Avenue, Beijing 100036, China.

## Abstract

The  $M_s$  8.0 Wenchuan earthquake of May 12, 2008 induces large-amplitude water level changes at intermediate and far fields (epicentral distance  $>1.5$  fault rupture length) in Chinese mainland. According to the seismograms, the co-seismic water level changes are attributed to the dynamic strain induced by the passage of seismic waves, most probably long period surface waves. Although many hydrologic changes induced by teleseismic waves have been reported, the mechanisms responsible for the changes still remain unclear. We invoke Skempton's coefficient  $B$  in this paper to explain those co-seismic water level changes documented in the intermediate and far fields. Some of those abrupt coseismic water level changes, for which the variation of the co-seismic water level, Skempton's coefficient  $B$  and the effective pressure preserve uniformity ( all increase or all decrease ) are found to favor the consolidation/dilatation induced by the shaking of teleseismic waves. While the other part of those coseismic water level changes, can be explained with the

24 enhanced permeability caused by fracture clearing or overcoming the capillary  
25 entrapment in porous channels of the aquifer induced by the shaking of teleseismic  
26 waves, and most of those wells lie in basins or in hollows, where the formation is  
27 relatively stable and stiff.

## 28 **Introduction**

29 Various hydrologic responses to earthquakes have been documented (Kayen *et al.*,  
30 2004; Elkhoury *et al.*, 2006; Sil and Freymueller, 2006; Chadha *et al.*, 2008;  
31 Wang and Manga, 2010), many occurred at great distances from the ruptured fault  
32 where static stress changes are relatively small. Hydrologic changes induced by  
33 teleseismic waves have been investigated in several studies of water wells (Roeloffs,  
34 1998; Brodsky *et al.*, 2003; Elkhoury *et al.*, 2006; Geballe *et al.*, 2011). Earthquake  
35 induced water level changes at distant locations were reported after the Denali  
36 earthquake (Brodsky *et al.*, 2003; Kayen *et al.*, 2004; Sil and Freymueller, 2006).  
37 Seismic oscillations, due primarily to surface waves from distant events, occur in  
38 some wells tapping highly transmissive aquifers (Liu *et al.*, 1989; Liu *et al.*, 2006). Sil  
39 and Freymueller (2006) developed an empirical relationship between water level  
40 changes, epicentral distances and earthquake magnitude in the far-field. Chadha *et al.*  
41 (2008) find wells appear to respond to regional strain variations and transient changes  
42 due to distant earthquakes. Liu and Manga (2009) indicate that significant water level  
43 changes can be driven at great distances by moderate-amplitude dynamic  
44 (time-varying) stresses.

45 Several mechanisms have been proposed to explain these co-seismic changes in  
46 water level. Fracture clearing and increased permeability caused by the  
47 earthquake-induced dynamic stress have been widely used to explain most

48 documented far-field water level changes (Brodsky *et al.*, 2003; Elkhoury *et al.*, 2006;  
49 Wang and Chia, 2008; Wang and Manga, 2010). Overcoming the capillary  
50 entrapment in porous channels is hypothesized to be one of the principal pore-scale  
51 mechanisms by which natural permeability is enhanced by the passage of elastic  
52 waves (Beresnev, 2011). Dynamic strain induced by the passage of seismic waves,  
53 most probably long period surface waves might be the cause of water level changes in  
54 the far-field (West *et al.*, 2005; Sil and Jeffrey, 2006; Chadha *et al.*, 2008). Other  
55 proposed, but also unverified mechanisms include pore pressure increases caused by a  
56 mechanism ‘akin to liquefaction’ (Roeloffs, 1998), shaking-induced dilatancy (Bower  
57 and Heaton, 1978), increasing pore pressure through seismically induced growth of  
58 bubbles (Linde *et al.*, 1994), and fracture of an impermeable fault (King *et al.*, 1999).  
59 In addition, Huang (2008) observed the co-seismic water level increase may be  
60 caused by the consolidation induced by the transmission of teleseismic waves in  
61 Fuxin well. Experimental measurements of Liu and Manga (2009) indicate that  
62 permeability changes (either increases or decreases) owing to dynamic stresses are a  
63 reasonable explanation. In general, they find permeability decreases after shaking.

64 In the present study, we use the Skempton’s coefficient  $B$ , the co-seismic water  
65 level and the inferred effective pressure to explain the co-seismic water level changes  
66 in the intermediate and far fields based on datasets from the Wenchuan earthquake in  
67 the Chinese mainland. Using a poroelastic relation between water level and solid tide  
68 (Zhang *et al.*, 2009), we calculate the in-situ Skempton’s coefficient  $B$  both pre and  
69 post earthquake (which are two independent quasistatic processes). From the  
70 research we find: Consolidation/dilatation induced by shaking of teleseismic waves,  
71 may account for the mechanism of those abrupt coseismic water level changes, for

72 which the variations of the co-seismic water level, Skempton's coefficient  $B$  and the  
73 effective pressure preserve uniformity. While, the other part of those coseismic water  
74 level changes, for which the co-seismic water level and the effective pressure change  
75 with inconformity (most of those wells stay in basins with relatively stable and stiff  
76 formations) may be explained with the increased permeability caused by teleseismic  
77 waves, which in turn lead to the redistribution of pore pressure. Compare the  
78 occurrence time of water level changes with the arrival time of surface waves in  
79 several stations, we find the co-seismic water level changes are induced by the long  
80 period surface waves.

## 81 Selection Principles and Observations

82 Large numbers of stations with co-seismic water level changes induced by  
83  $M_s$  8.0 Wenchuan earthquake have been collected in the intermediate and far fields  
84 ( $>1.5$  fault-rupture lengths). Most of those water level changes in this area can not be  
85 induced by the change of the static strains, which are extremely tiny (Zhang and  
86 Huang, 2011). We selected those co-seismic water level changes with distinct  
87 amplitude (tiny or obscured co-seismic water level changes have been excluded). In  
88 order to calculate the pre- and post- earthquake  $B$  values, water level data in stations  
89 should not be long-time missing or be influenced by other factors, such as pumping or  
90 other disturbances, and the data should be long enough (at least with a 10-day  
91 continuous data before and after the earthquake respectively), so that we can use the  
92 least-square fit to calculate  $B$  (Appendix). In addition, the oceanic tides has been  
93 known to have an effect several tens of kilometers away from the seashore (Beaumont  
94 and Berger, 1975). The deformation caused by ocean tide loading is difficult to  
95 calculate, these tides appear with the same frequencies as the solid earth effects (Khan

96 and Scherneck, 2003), and the tides are strongly affected by the complicated  
97 topography around the seashore (Walters and Goring, 2001), so we can't simply to  
98 calculate the oceanic tides by theory models. Besides, there are no public software to  
99 calculate the China national offshore ocean tides, so we have to delete those wells (4  
100 wells: Hejiazhuang, Huanghua, Wafangdianloufang and Yongchun) which may be  
101 influenced by the ocean tides seriously. Bearing those rules in mind, we find 11  
102 stations (well a to well k (Figure 1)) can be chosen during the Wenchuan earthquake  
103 (Table 1).

104 Detailed basic information of each well are show in Table 1 , including well  
105 depth, well diameter, aquifer lithology, and geological structure. However, diameter of  
106 well g, h and j can not be found. The detailed borehole columnar diagrams (borehole  
107 columnar diagram of well b, g, h, i, and j can not be found) are not show in this paper,  
108 those information obtained from the borehole columnar diagrams together with the  
109 aquifer lithology are show in Table 1. All the water level recording instruments in  
110 those wells (well a to well k) are digital, they are LN-3A digital water level  
111 instrument (except for Mile well it uses LN-4A digital water level instrument, and  
112 Fuxin well uses the SQ digital water level instrument), with the observation accuracy  
113  $\leq 0.2\%$  F.S. , and the sampling rate of 1/min, the resolution ratio is 1mm. We use the  
114 Mapseis software (Lu *et al.*, 2002) to calculate the tidal strain data (hourly data). In  
115 order to keep in accordance, both the water level and the tidal strain use the hourly  
116 data when calculating the Skempton's coefficient  $B$ .

## 117 **Intermediate and Far Field Analysis**

118 **Assumptions of shear modulus and Poisson's ratio and the calculation of**  
119 **Skempton's coefficient  $B$**

120 Calculations are performed using  $\rho = 1000 \text{ kg / m}^3$ ,  $g = 9.8 \text{ m / s}^2$ , and  $\nu_u = 0.29$   
121 according to equation (5) (Appendix). We suppose the undrained Poisson's ratio  
122  $\nu_u = 0.29$  both pre and after earthquake, and this kind of assumption is always used  
123 to simplify calculation issues of rocks near the crust (Zeng, 1984). In addition, based  
124 on the poroelastic theory, and limited to isotropic conditions, Theo *et al.*(2002) aim to  
125 determine the elastic material constants of the solid matrix with two level of porosities.  
126 As it is not possible to experimentally determine the elastic material constants of the  
127 solid matrix at these levels, a theoretical approach is presented, based on experimental  
128 data taken from literature. They find different porosities lead to different values of  
129 elastic modulus. Their results indicate that the variation extents of Skempton's  
130 coefficient  $B$  and the bulk modulus are much larger than the drained and undrained  
131 poisson's ratios (variation extent of  $B$ : 6.3% ; variation extent of  $K$ : 7.96% variation  
132 extent of  $\nu_u$ : 0.3% ). So we can approximately assume that compared to the  
133 variations of the porous medium modulus (the bulk modulus and Skempton's  
134 coefficient  $B$ ), the change of the undrained poisson's ratio can be neglected before and  
135 after the earthquake.

136 Gassmann (1951) predicted that the effective shear modulus would be  
137 independent of the saturating fluid properties (the shear modulus is a constant) in the  
138 undrained isotropic poroelastic media. As studied by Berryman (1999) and Berryman  
139 and Wang (2001), the theory applies at very low frequencies. At high enough  
140 frequencies (especially in the ultrasonic frequencies), as the numerical simulation of  
141 Berryman and Wang (2001) shows (based on the effective medium theory, and use a  
142 complete set of poroelastic constants for drained Trafalgar shale), with the increase of  
143 Skempton's coefficient  $B$ , the bulk modulus changes by as much as 100% in this  
144 example, whereas the shear modulus changes by less than 10%, and other rock



145 examples also show similar results (Berryman and Wang, 2001). As discussed above,  
146 we can know: It is obvious that the change of shear modulus  $G$  is tiny, and even can  
147 be neglected (both in the drained or undrained cases) as compared with the change of  
148 Skempton's coefficient  $B$ . In this paper we suppose, shear modulus of well aquifer  
149 systems will not change after affected by the seismic waves (the frequencies of  
150 seismic waves are much lower than the ultrasonic frequencies, so the change of the  
151 shear modulus will be neglectable compared to the change in  $B$  value).

152 We apply the  $B$ -calculation method (Appendix) to those well-picked stations.  
153 The pre-and post-earthquake  $B$  values are respectively obtained from May 1, 2008 to  
154 May 11, 2008, and from May 13, 2008 to May 24, 2008 (Figure 2).

### 155 **Undrained Skempton's coefficient $B$ as a function of effective pressure**

156 When the aquifer be consolidated, the effective pressure (effective pressure =  
157 confining pressure - pore pressure) will increase, while a dilation is in accordance to  
158 the decrease of effective pressure. Blocher *et al.* (2009) measured the relationship  
159 between Skempton's coefficient  $B$  and effective pressure based on the laboratory  
160 experiment. The in-situ aquifer of those wells (well a~k) we studied are under  
161 lithostatic pressures for a long time and also be affected by the transmission of  
162 seismic waves for countless times, the situation is much similar to those well bedrocks  
163 be applied on repeated pressure cycles. So the situation will be much similar to the  
164 last several ramps (apply more than once pressure cycles on the rock) rather than the  
165 first ramp (apply the first pressure cycle on the rock, during which a possible  
166 dissolution of gas in the fluid of an incompletely saturated sample happened) in the  
167 experiment of Blocher *et al.* (2009), and the isotropic Skempton's coefficient  $B$  will  
168 increase/decrease with the increase/decrease of effective pressure (when the effective

169 pressure is less than  $\sim 4$  Mpa), while  $B$  will decrease with the increase of effective  
170 pressure (when the effective pressure is larger than  $\sim 4$  Mpa). Although these results  
171 obtained from sandstone, because of the lack of the laboratory experiment study of  
172 those specific rocks, we assume the results can be applied to the bedrock of all those  
173 wells studied in this paper.

174 In order to compare with the experiment results, we have to estimate the  
175 effective pressure of each well. Pore pressure response to gravitational loading is  
176 similar to tectonic loading and can also be treated as a poroelastic problem (Green and  
177 Wang, 1986). Depths of those wells analyzed in this paper are all less than 1km  
178 (Table 1). W-1 well lies in Yanchang basin of Gansu province, Yanchang basin is a  
179 deep basin with Paleozoic sediments (Wu *et al.*, 2010). The “pressure - depth”  
180 relation of well W-1 (Figure 3a) is similar to other wells in the Chinese mainland. So  
181 we assume those results could be applied to these wells we studied (well a  $\sim$  k) since  
182 we lack the “pressure-depth” predictions of these wells. We calculate the effective  
183 pressure of W-1 well (effective pressure approximately equals to lithostatic pressure  
184 minus pore fluid pressure) (Figure 3b), and estimate the range of the effective  
185 pressure of these wells we studied according to the well-depth (Table 1).

186 We calculated the change of pore pressure in each well ( $\Delta P_p = \rho g \Delta h$ ), together  
187 with the range of the effective pressure, the variation trend of Skempton’s coefficient  
188  $B$ , and the  $B$ -effective pressure relation obtained by the experiment of Blocher *et al.*  
189 (2009), we can infer the variation of the effective pressure in each well (Table 2,  
190 Table 3). When the range of the effective pressure lies in 0-3 Mpa (most of the wells),  
191 the increase/decrease of  $B$  accompanied with the increase/decrease of effective

192 pressure. When the range of effective pressure  $>5$  Mpa, the increase/decrease of  $B$   
193 accompanied with the decrease/increase of effective pressure Blocher *et al.* (2009),  
194 only the effective pressure of Jurong well (well f) lies in this range (Table 3).

## 195 **Mechanism analysis**

### 196 **Coseismic water level change induced by consolidation or dilatation**

197 Water level increase/decrease accompanied with the increase/decrease of  
198 Skempton's coefficient  $B$  and the increase/decrease of effective pressure in well a, b,  
199 c, d, g, j, and k (Table 2). To our understanding, suppose the pressure not exceed a  
200 limitation (the fissures not be closed), when the aquifer be consolidated/ dilatated, the  
201 mean fracture width (the porosity and permeability) may decrease/increase with the  
202 increase/decrease of the effective pressure, then the stiff rock matrix that supports the  
203 load could with a higher/lower coupling to the fluid (Nur and Byerlee, 1971), and the  
204 value of  $B$  will increase/decrease. Hence, shaking induced by the transmission of  
205 teleseismic waves may cause consolidation/dilatation of the aquifer, and lead to the  
206 increase/decrease of the water level. Figure 4 shows the relation between the change  
207 of Skempton's coefficient  $B$  and the change of effective pressure (pore pressure/water  
208 level) in well a, b, c, d, g, j, and k . Approximately, it displays a linear relation.

### 209 **Coseismic water level change induced by increased permeability**

210 Water level decrease/increase accompanied with the increase/decrease of  
211 Skempton's coefficient  $B$  and the increases/decrease of effective pressure in well e, h,  
212 and i (Table 3). Fracture clearing (unclogging) and increased permeability may be  
213 used to explain this phenomenon. Since pore-pressure heterogeneity may be the norm

214 in the field, an enhancement of permeability among sites of different pore pressure  
215 may cause pore pressure to spread (Roeloffs, 1998; Brodsky *et al.*, 2003; Wang, 2007;  
216 Wang and Manga, 2010). Pore-pressure of those wells may be higher/lower than other  
217 places before the earthquake, an enhancement of permeability incurred by (for  
218 example) overcoming the capillary entrapment in porous channels induced by the  
219 passage of elastic waves will decrease/increase the pore-pressure in those wells (the  
220 pore-pressure will shift to/shift from other places), and water level will  
221 decrease/increase. Then the effective pressure will increase/decrease accompanied  
222 with the decrease/increase of pore-pressure (water level), so the Skempton's  
223 coefficient  $B$  increase (which indicates the stiff rock matrix could with a higher  
224 coupling to the fluid) in well e, and decrease (which indicates the stiff rock matrix  
225 could with a lower coupling to the fluid) in well h and i (Table 3).

226 The depth of well f (889.18 m) is larger than other wells, and the effective  
227 pressure range of this depth is 8 ~ 10 MPa (Table 3 ). Effective pressure decreases  
228 accompanied with the Skempton's coefficient  $B$  increases in this range (Blocher *et al.*,  
229 2009). So water level increases with the decreases of effective pressure in this well,  
230 and this should be explained with the increased permeability. Pore-pressure of well f  
231 may be lower than other places before the earthquake, an enhancement of  
232 permeability will increase the pore-pressure in this well (the pore-pressure may shift  
233 from other places), and water level will increase. Then the effective pressure will  
234 decrease accompanied with the increase of pore-pressure, so the Skempton's  
235 coefficient  $B$  increase.

236 The local geological structure of each well is important (Table 1), we find that  
237 most of those wells in which permeability increase induced by shaking of teleseismic  
238 waves, stay in basins or in hollows (well e, f, h, i and Fuxin). Due to the mechanical

239 structure, the formation of the basin (or hollow) is relatively solid and stiff, and the  
240 deformation (consolidation or dilatation) will not easily to be incurred, then the  
241 energy of shaking may be inclined to induce the fracture clearing (unclogging) so as  
242 to increase permeability.

### 243 **Examples support far field water level increases induced by consolidation**

244 The spreading of teleseismic waves may cause dilatation of the aquifer medium,  
245 which can broaden the porosities and give birth to new fractures, and the effective  
246 pressure will reduce (in wells: g, j and k, the effective pressure range is 0 ~ 3 MPa)  
247 leading to the decrease of Skempton's coefficient  $B$ . This explanation is similar to the  
248 mechanism of shaking-induced dilatancy (Bower and Heaton, 1978). So it may be  
249 easier to understand water level decreases in the far field induced by the transmission  
250 of teleseismic waves. However, water level increases induced by consolidation in the  
251 far field is not the mainstream view. Since many cases support the theory of the  
252 increased permeability, it is necessary to give some examples which can support far  
253 field water level increases induced by consolidation.

254 Permeability will increase/decrease, which is mostly related to the  
255 increase/decrease of porosity (Xue, 1986). As explained by rock mechanics the same  
256 porosity always corresponding to the same effective pressure (Terzaghi, 1925;  
257 Magara, 1978). From that we can know porosity and permeability are all directly  
258 connected with effective pressure, and they will decrease with the increase of the  
259 effective pressure (Blocher *et al.*, 2009).

260 From the laboratory experiment, Liu and Manga (2009) find that: in general,  
261 permeability decreases after shaking. They measured the evolution of permeability in  
262 fractured sandstone in response to repeated shaking under undrained conditions, and

263 set the frequency and amplitude of the imposed shaking to be representative of those  
264 that cause distant hydrological responses. As they explained: Dynamic strains cause  
265 time varying fluid flow that can redistribute particles within fractures or porespace,  
266 and can allow particles to move away from regions where they hold pore spaces open,  
267 and are expected to accumulate and get trapped at the narrowest constrictions along  
268 flow paths, and hence allow a consolidation (contraction) of the sample. Their result  
269 just supports our mechanism analysis. It implies that teleseismic waves can cause a  
270 consolidation of well aquifer and cause the increase of effective pressure, which is in  
271 accordance with the increase of co-seismic water level changes accompanied with the  
272 increase of Skempton's coefficient  $B$  in wells: a, b, c, d ( effective pressure range 0 ~  
273 3 MPa ).

274 In addition, [Huang \(2008\)](#) find that: the water level increase in Fuxin well  
275 (1409.98 km away from Wenchuan, the well depth is 60.74 m, stiff Granite with a  
276 little basalt is the bedrock and we assume the shear modulus = 60 Gpa) is induced by  
277 the increase of volume strain (consolidation) ([Figure 5a](#)). In the Chinese mainland,  
278 Fuxin is the only well in which there are observations of volume strain and water  
279 level in a specific aquifer medium, and both of them show obvious co-seismic  
280 responses to Wenchuan earthquake. There are clear and obvious effects of tidal strain  
281 and atmospheric pressure in the water level and volume strain, which indicates Fuxin  
282 is a terrific artesian well. This well has not be chosen in the above analysis because  
283 there is an abrupt large-amplitude increase in the water level, which starts from 11  
284 p.m. May 22, 2008 (we can not find any interference of this abrupt increase according  
285 to the daily records of Fuxin station), and we can just use a shorter time period to  
286 calculate the post-earthquake  $B$  value, which may cause a little impact on the precise

287 of  $B$ . The calculation is performed based on the  $M_2$  wave distilled from the water  
288 level and the tidal strain (pre-earthquake: from May 1, 2008 to May 11, 2008,  
289 post-earthquake: from May 13, 2008 to May 22, 2008 (Figure 5b)). (The large-step  
290 abrupt water level increase starts from 09 p.m. May 22, 2008 (Figure 5c), which may  
291 cause large impact on the detrend process and influence the calculation result, so we  
292 discard these data). From Figure 5a, we can see the co-seismic water level increase is  
293 induced by the change of the volume strain, which indicates the well aquifer has been  
294 consolidated. The depth of Fuxin well is 60.74 m, and we can assume the range of the  
295 effective pressure is 0~3Mpa (Table 3), from the change of the pre- and post-  
296 earthquake  $B$  (Figure 5b), we may infer the consolidation may be very extreme,  
297 accompanied with the coseismic water level increase it could cause an extra pressure,  
298 which overcomes the capillary entrapment in porous channels of the aquifer or incurs  
299 a fracture clearing and bring in the increase of the permeability, then water flow in  
300 from other places with a higher pressure, which lead to the decrease of the  
301 Skempton's coefficient  $B$  with the decrease of the effective pressure, and the water  
302 level increases more gradually. Finally with the further enhancement of the  
303 permeability (increase of the porosity), a permanent deformation could be induced, so  
304 there is an abrupt increase in the water level in 22 May, and remain in a relatively  
305 high level for several months(Figure 5c). From the picture we can see it may be in a  
306 drained condition after the abrupt large-amplitude water level increase, because the  
307 water level fluctuates irregularly.

308 So we argue that water level increase induced by the consolidation incurred by  
309 transmission of teleseismic waves is reasonable, and in a specific geology condition,  
310 a consolidation with large enough energy may also lead to an enhanced permeability  
311 by fracture clearing or by overcoming the capillary entrapment in porous channels.

312 **Wellbore storage effects**

313 Tidal phase lags are caused by wellbore storage. “Wellbore storage” is the term  
314 used to describe a lag of piezometer water level behind aquifer pressure resulting  
315 from the need for water to flow into the borehole in order to equilibrate water level  
316 with aquifer pressure. Wellbore storage effects increase (phase lags increase) as the  
317 transmissivity (and permeability) of the formation decreases (Roeloffs, 1996; Doan *et*  
318 *al.*, 2006).

319 Most of those wells can record clear tidal strain and atmospheric pressure, and  
320 according to the <China earthquake monitoring records series> (which is written by  
321 different Subordinate units (earthquake administration of each provinces and different  
322 institutions) of China Earthquake Administration, and published in Beijing in  
323 different years by Seismological Press (in Chinese)) they are well confined. From  
324 [Table 1](#) we can see the phase difference of water level and tidal strain of most wells  
325 are 0, which mean good correlations between the water levels and the tidal strains,  
326 and those wells are well confined and under the undrained condition. Because we use  
327 the hourly data, we can not identify the phase difference when it is less than 1 hour,  
328 and we just neglected the wellbore storage effects in those wells. Before and after the  
329 earthquake, if phase lags remain the same, it indicates the permeability of the well  
330 aquifer keeps the same or just changes a little (the phase difference may be less than 1  
331 hour). Phase lags  $\geq 1$  hour in well: b, c, e, and Fuxin, and most of them are small,  
332 except well b, which may be semi-confined. Thus, the validity of the calculated  $B$   
333 values in well b may be a little questionable. The phase lag of Fuxin well decreases  
334 after the earthquake ( $L_1=2$  hours,  $L_2=1$  hour), which indicates the permeability  
335 increases after the shaking of the earthquake, this is in accordance with the mechanism  
336 analysis of the co-seismic water level increase in Fuxin well.



## 337 **Discussion**

### 338 **The variation of porosity**

339 [Figure 3c](#) shows, in general, the porosity decreases with the increase of depth,  
340 however, when reach 3000m the effective pressure turns much larger (approximately  
341 equals to 35 Mpa) than that in the depth of those wells (well a ~ k), the porosity still  
342 persists relatively large, and changes with different depth. From [Table 2](#) we can see,  
343 the variation of effective pressure of well a, b, c, d, g, j and k is less than 0.01Mpa,  
344 and from [Figure 3b](#) we know, variation of 0.01Mpa in effective pressure  
345 approximately equals to variation of 1 meter in depth, as [Figure 3c](#) shows, the  
346 variation of porosity is tiny during variation of 1 meter in depth. So this variation  
347 extent of effective pressure is hard to induce permanent deformation of porosity.  
348 However, in reality, the change of porosity may also connected with the formation  
349 and the state of the rock matrix.

350 Furthermore, phase lags of well a, b, c, d, g, j and k keep constant before and  
351 after the earthquake (change less than 1 hour) ([Table \(1\)](#)), so we can infer, the  
352 porosity (permeability) change little after the earthquake. Because the phase lags  
353 increase/decrease (wellbore storage effects increase/decrease) as the permeability  
354 (porosity) of the formation decreases/increase ([Roeloffs, 1996; Doan et al., 2006](#)).

355 So we can infer, the porosity of well a, b, c, d, g, j and k can persist despite being  
356 reduced/enlarged due to the consolidation/dilatation induced by the passage of  
357 teleseismic waves of  $M_s$  8.0 Wenchuan earthquake.

### 358 **Uncertainty of $B$ coefficient**

359 In order to study the uncertainty of  $B$  coefficient (error related to the

360 determination of  $B$  coefficient), we use Jurong well to show the variation of  $B$  during  
361 a relatively long – time span (50 days before and after the Wenchuan earthquake)  
362 (Figure 6). Skempton’s coefficient  $B$  will change with the change of time. Because we  
363 use the least square fit to calculate  $B$ , the value may be a little different when we use  
364 different length of data , but the change tendency (increase or decrease of  $B$ ) before  
365 and after the earthquake will be constant. Furthermore, we can see the  $B$  value of  
366 Jurong well recover to its initial value after about 30 days (Figure 6).

367 So, compared with the uncertainty in  $B$  value, variation of  $B$  due to the  
368 earthquake is significant. The continuous of  $B$  will be influenced by lots of factors,  
369 such as power off, aftershocks, and so on, so  $B$ -value series at large time scale is not  
370 easy to obtain for each well.

### 371 **Recovery of Water level**

372 The recovery time of the water level is obscure, because most of those water  
373 level will not recover to the same height as the pre-earthquake level during a  
374 relatively short time span. So we should use much longer data to analyze it, and  
375 should discard all those influences: such as aftershocks, atmospheric pressure ( not all  
376 those wells have the records of atmospheric pressure ) , tidal strain, pumping, power  
377 off, thunder and so on, which needs lots of work, and we may study about it in future.  
378 In addition, we haven’t find any relation between water level changes and epicentral  
379 distances in those wells studied in this paper, it is possible to investigate much more  
380 wells later, to study about the relations.

### 381 **The variation value of effective pressure**

382 We calculated the change of pore pressure ( $\Delta p_p = \rho g \Delta h$ ), and we can use the

383 critical state to help us to analyze the variation value of effective pressure in each  
384 well.

385 When the aquifer be consolidated/dilated, in the critical state, the pore pressure  
386 keeps constant, the confining pressure increase /decrease, then the effective pressure  
387 increase/decrease, and at last transfer into the increase/decrease of pore pressure  
388 (water level increase/decrease), and the system comes into an equilibrium state. So the  
389 change of pore pressure can be attributed to the change of the effective pressure.

390 When the permeability increase, in the critical state, the confining pressure keeps  
391 constant, the pore pressure (water level) increase (the well in a relatively low pressure  
392 region before the earthquake) /decrease (the well in a relatively high pressure region  
393 before the earthquake), then the effective pressure decrease/increase, so the change of  
394 the effective pressure can be attributed to the change of pore pressure.

395 However , the variation value of the effective pressure of each well may be  
396 different from the value we calculate, because the critical state is an assumption ideal  
397 state, and the transfer of stress may also relate with the formation and state of the  
398 aquifer.

### 399 **Compare with seismograms**

400 There are 48 national stations recording the seismograms (event waveforms) in  
401 the Chinese mainland (we can not obtain the regional seismograms because of the  
402 authority limitation), however most of those stations are not in the same place with  
403 stations which have the records of water level changes. Those stations (well a to k)  
404 analyzed in our paper have no records of seismograms. After comparison, generally  
405 we may use the seismograms of 4 national stations to analyze the corresponding water

406 level observations (Figure 7), which are near those national stations (the distances  
407 between the water level wells and the national seismogram stations are approximately  
408 less than 100km). We use the seismogram of Sheng yang (SNY) national station to  
409 analyze Fuxin well (there are about 102.81 km between them), while Taiyuan (TIY)  
410 national station is corresponding to well e (there are about 40.903 km between them);  
411 Lanzhou (LZH) station is corresponding to well g (there are about 19.82 km between  
412 them); and Hefei (HEF) station is corresponding to well k (there are about 91.57 km  
413 between them). In addition, the geology conditions are very similar (the main bed  
414 rock of Fuxin well and Shengyang station are both granite; Well e is in the east of  
415 Taiyuan basin, bed rock of well e and Taiyuan station are both limestone; Well k is in  
416 Chuhe river major dislocation and Hefei--Dongguan fracture intersection; bed rock of  
417 well g and Lanzhou station are both sandstone).

418 However, because the Z-component seismogram of TIY national station is  
419 deficient, we have to give up the analysis of Z component in TIY station. The  
420 waveforms in LZH station is also deficient, there may be some disturbances (Figure  
421 7). There are only hourly water level data in Fuxin well (minute data observation  
422 strats from 2009), so we can not use that to do precise comparison (in minute) with  
423 the seismogram. In general, we can only use well e and well k to do the comparisons  
424 between the timing of steps in water level changes and the arrival time of waves in  
425 seismograms.

426 From the occurrence time of water level changes and the arrival time of surface  
427 waves of well e and well k (Table 4), we find the co-seismic water level changes are

428 attributed to the passage of surface waves in the two wells. From that, we may infer:  
429 in other wells the co-seismic water level changes are attributed to the dynamic strain  
430 induced by the passage of teleseismic waves, most probably surface waves, which  
431 have relatively larger amplitude of oscillation, corresponding to relatively larger  
432 energy. The similar conclusion has been proposed by [Sil and Jeffrey \(2006\)](#), [West \*et al.\* \(2005\)](#), and [Chadha \*et al.\* \(2008\)](#).

434 Since well g and well k are all induced by the dilatations incurred by teleseismic  
435 waves, we can do some comparisons between them. From the seismograms we can  
436 see, the velocity amplitude of LZH (near well g) is much larger than that of HEF (near  
437 well k), so the energy of the teleseismic waves is much larger in well g than in well k  
438 (energy is in direct proportion to the square of the amplitude of oscillation). However,  
439 the amplitude of the co-seismic water level changes are not only related to the energy,  
440 but also connected with the different local geology conditions, such as the extent of  
441 the coupling between the solid matrix and the fluid (Skempton's coefficient  $B$  ( $B$   
442 value of well k is larger than that of well g)), so the amplitude of the coseismic water  
443 level change of well k is larger than that of well g.

444 Because of the low temporal resolution of the water level data, further analysis of  
445 the steps could not be made. Co-seismic water level changes occurred in the 2 wells  
446 (well e and well k) during the passage of surface waves. More precise estimation of  
447 the timing of the step could not be made because of the low temporal resolution of the  
448 water level data. Obviously, there are geographic position difference between the  
449 observation of seismograms and water levels, and there are also some errors on the

450 manual amplitude readings, both of which could cause some influence on the analysis.

451 From the geological structures, we find that most of those wells in which  
452 permeability increase induced by shaking of teleseismic waves, stay in basins or in  
453 hollows (well e, f, h, i and Fuxin), which may be attributed to the relatively stiff  
454 formation of those basins or hollows due to the mechanical structure. According to the  
455 the diverse and very complicated geology conditions, we may focus on 1—2 wells  
456 (which record both the water level and the seismogram), to do much more deeply  
457 analysis in future, so as to reveal the mechanism more deeply and clearly.

## 458 **Conclusion**

459 Together with the variation of Skempton's coefficient  $B$ , the change of pore  
460 pressure and the inferred variation of effective pressure in each well, we can infer the  
461 mechanism of the co-seismic water level changes. From the study we can conclude:  
462 consolidation/dilatation induced by shaking of teleseismic waves, may account for the  
463 mechanism of those abrupt coseismic water level changes, for which the variation  
464 tendency of the co-seismic water level, Skempton's coefficient  $B$  and the effective  
465 pressure keep the same (all increase or all decrease). While, fracture clearing and  
466 increased permeability may be used to explain the other part of those coseismic water  
467 level changes, for which the co-seismic water level, and the effective pressure change  
468 with inconformity, and most of those wells stay in basins with relatively stable and  
469 stiff formations. Compared with the seismograms, the co-seismic water level changes  
470 are attributed to the dynamic strain induced by the passage of seismic waves, most  
471 probably long period surface waves. Our analysis is not conflict with any of those  
472 existing theories. Although those water level changes happened in the intermediate

473 and far fields, most of those water levels present abrupt and obvious co-seismic  
474 changes owing to the huge energy of  $M_s$  8.0 Wenchuan earthquake.

475 From the analysis of Fuxin well, we can see a consolidation with large enough  
476 energy may overcome the capillary entrapment in porous channels or clear the  
477 fractures, and incur an enhanced permeability. So as discussed by Liu and Manga  
478 (2009), permeability changes (either increases or decreases) owing to dynamic  
479 stresses are reasonable explanations for earthquake-induced hydrologic responses.  
480 The mechanisms analyzed in this paper are similar to the experiment results of Liu  
481 and Manga (2009), and our in-situ analysis may complement the limitation of the  
482 initial condition of their laboratory experiments.

483 In reality, the shear modulus  $G$  and the undrained Poisson's ratio  $V_u$  would  
484 change slightly after the shaking of seismic waves, and the discussed "undrained"  
485 condition can hardly last for a long time, as long as the fluid flow exists, the  
486 undrained condition will disrupt and be replaced by the drained condition soon. We  
487 assume the results get from sandstone can be applied to all those bedrocks in those  
488 wells (Figure 3), however this is not very precise. As described by Wang (1993)  
489 nonlinear compaction effects can be significant and they are not incorporated in the  
490 linear theory presented here, because the well aquifers are under lithostatic pressures  
491 for a long time and withstand large numbers of seismic shaking, the irreversible  
492 deformations and the nonlinear effects have been minimized (In the laboratory  
493 experiment, in order to reduce the irreversible deformation and to minimize the  
494 nonlinear effects, repeated pressure cycles are always applied on rock samples as  
495 preconditions (Blocher *et al.*, 2009)). Discard all those ideal assumptions, things may  
496 be different.

## 497 **Data and Resources**

498 Data used in this paper were collected using a classified network (Groundwater  
499 Monitoring Network, GMN) of the China Earthquake Networks Center and cannot be  
500 released to the public. We use the Mapeis software (Lu *et al.*, 2002) to calculate the  
501 tidal strain data.

502 **Acknowledgements.** We thank professor Emily Brodsky and postdoctor  
503 Jinlai Hao for discussion and help on this paper. This research was supported by the  
504 Natural Science Foundation of China (Grant No. 40925013 and 41040036). We  
505 gratefully appreciate the valuable suggestions proposed by the anonymous reviewers.

## 506 **Reference**

- 507 Brodsky, E., E. Roeloffs, D. Woodcock, I. Gall, and M. Manga (2003). A mechanism  
508 for sustained groundwater pressure changes induced by distant earthquake, *J.*  
509 *Geophys. Res.* **108(B8)**, 2390.
- 510 Beresnev, I., W. Gaul, and R. D. Vigil (2011). Direct pore-level observation of  
511 permeability increase in two-phase flow by shaking, *Geophys. Res. Lett.* **38**,  
512 L20302.
- 513 Blocher G., G. Zimmermann and H. Milsch (2009). Impact of poroelastic response of  
514 sandstone on geothermal power production, *Pure appl. geophys.* **166**,  
515 1107–1123.
- 516 Bower, D. R., and K. C. Heaton (1978). Response of an aquifer near Ottawa to tidal  
517 forcing and the Alaskan earthquake of 1964, *Can. J. Earth Sci.* **15**, 331–340.
- 518 Berryman, J. G., and H. F. Wang (2001). Dispersion in poroelastic systems, *Phys. Rev.*  
519 *E* **64**, 011303.
- 520 Berryman, J. G. (1999). Origin of Gassmann's equations, *Geophysics* **64**, 1627–1629.



- 521 Beaumont, C. and J. Berger (1975). An analysis of tidal strain observations from the  
522 United States of America: I. The laterally homogeneous tide, *Bull. Seismol. Soc.*  
523 *Am.* **65**, 1613–1629.
- 524 Chadha, R. K., C. Singh, and M. Shekar (2008). Transient changes in well-water level  
525 in bore wells in western India due to the 2004 Mw 9.3 Sumatra Earthquake,  
526 *Bull. Seismol. Soc. Am.* **98**, 2553–2558.
- 527 Chadha, R. K., H. J. Kuempel and M. Shekar (2008). Reservoir triggered seismicity  
528 (RTS) and well water level response in the Koyna-Warna region, India.  
529 *Tectonophysics* **456**, 94–102.
- 530 Doan, M. L., E. E. Brodsky, R. Prioul and C. Signer (2006). Tidal analysis of  
531 borehole pressure-A tutorial, *Schlumberger Research report*, P35.
- 532 Elkhoury, J. E., E. E. Brodsky and D. C. Agnew (2006). Seismic waves increase  
533 permeability, *Nature* **411**, 1135–1138.
- 534 Green, D. H. and H. F. Wang (1986). Fluid pressure response to undrained  
535 compression in saturated sedimentary rock, *Geophysics* **51(4)**, 948–956.
- 536 Geballe, Z. M., C.-Y. Wang, and M. Manga (2011). A permeability-change model for  
537 water-level changes triggered by teleseismic waves, *Geofluids* **11**, 302–308.
- 538 Gassmann, F. (1951). Über die elastizität poröser medien, *Vierteljahrsschrift der*  
539 *Naturforschenden Gesellschaft in Zürich*, **96**, 1–23.
- 540 Huang, F.-Q. (2008). *Response of Wells in Groundwater Monitoring Network in*  
541 *Chinese Mainland to Distant Large Earthquakes*, [Ph.D Dissertation] Institute  
542 of Geophysics, China Earthquake Administration, Beijing, pp. 47, (in Chinese).
- 543 Kan, S. A., and H. G. Scherneck (2003). The M2 ocean tide loading wave in Alaska:

544 vertical and horizontal displacements, modelled and observed, *J. Geodesy* **77**,  
545 117–127.

546 Kayen, R. E., E. Thompson, D. Minasian, R. E. S. Moss, B. D. Collins, N. Sitar, D.  
547 Dreger, G. A. Carver (2004). Geotechnical reconnaissance of the 2002 Denali  
548 Fault, Alaska, Earthquake. *Earthq. Spectra* **20**, 639–667.

549 King, C.-Y., S. Azuma, G. Igarashi, M. Ohno, H. Saito, and H. Wakita (1999).  
550 Earthquake-related water-level changes at 16 closely clustered wells in Tono,  
551 central Japan, *J. Geophys. Res.* **104**, 13,073–13,082.

552 Linde, A. T., I. S. Sacks, M. J. S. Johnston, D. P. Hill, and R. G. Bilham (1994).  
553 Increased pressure from rising bubbles as a mechanism for remotely triggered  
554 seismicity, *Nature* **371**, 408–410.

555 Liu, W. Q., M. Manga (2009). Changes in permeability caused by dynamic stresses in  
556 fractured sandstone, *Geophys. Res. Lett.* **36**, L20307.

557 Liu, C., M. W. Huang, and Y. B. Tsai (2006). Water level fluctuations induced by  
558 ground motions of local and teleseismic earthquakes at two wells in Hualien,  
559 eastern Taiwan, *TAO* **17**, 371–389.

560 Liu, L.B., E. Roeloffs, and X. Y. Zheng (1989). Seismically induced water level  
561 fluctuations in the WaliWell, Beijing, China, *J. Geophys. Res.* **94**, 9453–9462.

562 Lu, Y. Z., S. L. Li, Z. H. Deng, H. W. Pan, S. Che, and Y. L. Li (2002). *Seismology*  
563 *Analysis and Prediction System Based on GIS (Mapseis Software)*, Chengdu  
564 Map Press, Chengdu, China, 232.

565 Magara, K. (1978). Compaction and fluid migration, *Practical petroleum geology*.

566 Amsterdam: Elsevier Scientific Publishing Company, 1–319.

567 Nur, A., and J. Byerlee (1971). An exact effective stress law for elastic deformation of  
568 rocks with fluids, *J. Geophys. Res.* **76**, 6414–6419.

569 Rice, J. R., and M. P. Cleary (1976). Some basic stress diffusion solutions for fluid-  
570 saturated elastic porous media with compressible constituents, *Rev. Geophys.* **14**,  
571 227–241.

572 Roeloffs, E. A. (1996). Poroelastic techniques in the study of earthquakes-related  
573 hydrologic phenomena, *Adv. Geophys.* **37**, 135–195.

574 Roeloffs, E. A. (1998). Persistent water level changes in a well near Parkfield,  
575 California, due to local and distant earthquakes, *J. Geophys. Res.* **103**, 869–889.

576 Sil, S. (2006). Response of Alaskan wells to near and distant large earthquakes,  
577 Master’s Thesis, University of Alaska Fairbanks, pp. 8–11.

578 Sil, S. and J. T. Freymueller (2006). Well water level changes in Fairbanks, Alaska,  
579 due to the great Sumatra-Andaman earthquake, *Earth Planets Space* **58**,  
580 181–184.

581 Terzaghi, K. (1925). Principles in soil mechanics, III. Determination of the  
582 permeability of clay, *Engineering News Record.* **95**, 832–836.

583 Theo, H. S., M. H. Jacques, and C. C. Stephen (2002). Estimation of the poroelastic  
584 parameters of cortical bone, *J. Biomech.* **35**, 829–835.

585 Wang, H. F. (2000). *Theory of linear poroelasticity with application to geomechanics*  
586 *and hydrogeology*. Princeton University Press, Princeton, pp. 5–6.

587 Wang, H. F. (1993). Quasi-static poroelastic parameters in rock and their geophysical  
588 applications, *PAGEOPH* **141**, 269–286.

589 Wang, C.-Y. (2007). Liquefaction beyond the near field, *Seismol. Res. Lett.* **78**,  
590 512–517.

591 Wang, C.-Y., and M. Manga (2010). *Earthquakes and Water, Series: Lecture Notes in*  
592 *Earth Sciences*. Springer Press, Berlin, pp. 18–24.

593 Wang, C.-Y., and Y. Chia (2008). Mechanism of water level changes during  
594 earthquakes: Near field versus intermediate field, *Geophys. Res. Lett.* **35**,  
595 L12402.

596 Walters, R. A. and D. G. Goring (2001). Ocean tides around New Zealand, *New. Zeal.*  
597 *J. Mar. Fresh.* **35**, 567–579.

598 Wu, H. Z., L. Y. Fu and H. K. Ge (2010). Quantitative analysis of basin-scale  
599 heterogeneities using sonic-log data in the Yanchang Basin, *J. Geophys. Eng.* **7**,  
600 41–50.

601 West, M., J. Sanchez, and S. McNutt (2005). Periodically-triggered seismicity at Mt.  
602 Wrangell volcano following the Sumatr earthquake, *Science*, **308**,1144–1146.

603 Xue, Y.-Q. (1986). *Groundwater dynamics*. Geology Press, Beijing, pp. 16, (in  
604 Chinese).

605 Zhang, Y., F. Q. Huang, and G. J. Lai (2009). Research on Skempton’s coefficient *B*  
606 based on the observation of groundwater of Changping station, *Earthq. Sci.* **22**,  
607 631–638.

608 Zhang, Y., and F. Q. Huang (2011). Mechanism of Different Coseismic Water-Level  
609 Changes in Wells with Similar Epicentral Distances of Intermediate Field, *Bull.*  
610 *Seismol. Soc. Am.* **101**, 1531–1541.

611 Zeng, R. S. (1984). *Solid Geophysics Introduction*, Press of Science, Beijing, pp. 9,  
612 (in Chinese).

613 Zhao L. F., X. B. Xie, W. M. Wang, and Z. X. Yao (2008). Regional Seismic  
614 Characteristics of the 9 October 2006 North Korean Nuclear Test, *Bull. Seismol.*  
615 *Soc. Am.* **98**, 2571–2589.

616

### 617 **Appendix: An approach to Skempton's coefficient $B$ based on the** 618 **poroelastic theory**

619 Skempton's coefficient  $B$  is a significant pore-fluid parameter in poroelastic  
620 theory. A poroelastic material consists of an elastic matrix containing interconnected  
621 fluid saturated pores. Fluid saturated crust behaves as a poroelastic material to a good  
622 degree of approximation.

623 [Rice and Cleary \(1976\)](#) summarized the following equations for a linearly elastic  
624 isotropic porous medium (they are the building blocks of the poroelastic theory):

$$625 \quad 2G\varepsilon_{ij} = \sigma_{ij} - \frac{\nu}{1+\nu} \sigma_{kk} \delta_{ij} + \frac{3(\nu_u - \nu)}{B(1+\nu)(1+\nu_u)} p \delta_{ij}, \quad (1)$$

$$626 \quad m - m_0 = \frac{3\rho(\nu_u - \nu)(\sigma_{kk} + 3p/B)}{2GB(1+\nu)(1+\nu_u)}. \quad (2)$$

627 Here  $m - m_0$  is the change of the fluid mass,  $\varepsilon_{ij}$  is the strain tensor,  $\sigma_{ij}$  is the stress  
628 tensor,  $\delta_{ij}$  is the Kronecker delta function,  $G$  is the shear modulus,  $\rho$  is the  
629 density of the fluid,  $B$  is the Skempton's coefficient,  $p$  is the pore pressure,  $\nu$  is  
630 the Poisson's ratio, and  $\nu_u$  is the "undrained" Poisson's ratio. [Rice and Cleary \(1976\)](#)  
631 describe equation (1) as a stress balance equation and equation (2) as a mass balance  
632 equation.

633 For the undrained condition, the poroelastic effect on the crust can be obtained  
634 by putting  $m - m_0 = 0$  in equation (2) to obtain

$$635 \quad p = -B\sigma_{kk} / 3 \quad \text{or} \quad \Delta p = -B\Delta\sigma_{kk} / 3. \quad (3)$$

636 Equation (3) indicates that, in the undrained condition, the change in fluid pressure  
637 ( $\Delta p$ ) is proportional to the change in mean stress ( $\Delta\sigma_{kk} / 3$ ). This is the mechanism of  
638 water level changes for poroelastic material. ( $p = \rho gh$ , where  $h$  is the water column  
639 height,  $g$  is the acceleration due to gravity and  $\rho$  is the density of water).

640 According to equation (3), Skempton's coefficient  $B$  can be qualitatively defined:  
641 In the undrained condition,  $B$  is the ratio of the induced pore pressure divided by the  
642 change in mean stress (Wang, 2000).  $B$  governs the magnitude of water-level changes  
643 due to an applied stress because pore pressure is directly proportional to water level.  
644 The value of  $B$  is always between 0 and 1. When  $B$  is 1, the applied stress is  
645 completely transferred into changing pore pressure. When  $B$  equals 0, there is no  
646 change in pore pressure after applying the stress. Thus a low value of  $B$  indicates the  
647 stiff rock matrix that supports the load with low coupling to the fluid (Nur and  
648 Byerlee, 1971). Laboratory studies indicate the value of  $B$  depends upon the fluid-  
649 saturated pore volume of the sample (Wang, 2000).

650 Equation (3) can be expressed in terms of tidal strain as well (Roeloffs, 1996):

$$651 \quad \Delta h = -\frac{2GB(1 + \nu_u)}{3\rho g(1 - 2\nu_u)} \Delta \varepsilon_t. \quad (4)$$

652 Equation (4) shows that water level changes proportionally in a poroelastic material  
653 under the influence of tidal strain ( $\varepsilon_t$ ). Here,  $\Delta h$  is the change in height of water  
654 level, and  $\Delta \varepsilon_t$  is the corresponding tidal strain change (Sil, 2006).

655 From equation (4) we obtain:

656 
$$B = -\frac{3\rho g(1-2\nu_u)}{2G(1+\nu_u)} \frac{\Delta h}{\Delta \varepsilon_t}. \quad (5)$$

657 With equation (5), we obtain the value of  $B$  with water level and tidal strain. However,  
 658 the calculation must be on the strict premise of the undrained condition (the good  
 659 correlation between the water level and the tidal strain) and should not be influenced  
 660 by the other factors.

661 For the effect of the solid tide on the crust, when the wavelength of the tidal  
 662 strain is much larger than the size of the aquifer, we can suppose the aquifer system is  
 663 undrained (Huang, 2008). So we can suppose the effect of the  $M_2$  wave in the crust  
 664 can meet the undrained condition (Zhang *et al.*, 2009). In addition, those wells can  
 665 record clear tidal strains and thus, because we calculate the phase lags between the  
 666 water levels and the tidal strains are small, the wells can readily meet the undrained  
 667 condition. In the  $M_2$ - wave frequency domain, the water level and the tidal strain  
 668 show a good correlation; Furthermore, the  $M_2$  wave is hardly influenced by  
 669 atmospheric pressure. We therefore distill the frequency domain of the  $M_2$  wave  
 670 from the water level and the tidal strain by using band-pass filter (the frequency of the  
 671  $M_2$  wave is  $2.23636 \times 10^{-5} \text{ HZ}$  ) to calculate the Skempton's coefficient  $B$ . By  
 672 converting the frequency domain of the  $M_2$  waves (obtained from the water level and  
 673 the tidal strain), by inverse fast Fourier transform and adjusting their phases (using the  
 674 least-square fit and putting the results into equation (5)), we can finally derive  $B$ .  
 675 (More details of the method are explained in Zhang *et al.*, 2009). All the Water-level  
 676 observations come from the sensor of water level, while tidal strain data are calculated  
 677 via Mapseis software (see Data and Resources section). One thing needs to be  
 678 clarified: We haven't applied the static equations directly to relate pore pressure

679 changes to seismic waves. We use those static equations for the impact of the tidal  
680 strain on the aquifer medium before and after the Wenchuan earthquake, so as to  
681 obtain the pre- and post- earthquake Skempton's coefficient  $B$  (those two periods can  
682 be recognized as two independent quasi-static processes), so the poroelastic static  
683 equations can be applied.



1                   Studies of mechanism for water level changes induced by  
2                                           teleseismic waves

3       Yan Zhang<sup>1</sup>, Li-Yun Fu<sup>1</sup>, Fuqiong Huang<sup>2</sup>, Yuchuan Ma<sup>2</sup>, Lian-feng Zhao<sup>1</sup>, and Bo  
4                                           Zhao<sup>2</sup>

5       1. Key Laboratory of the Earth's Deep Interior, Institute of Geology and Geophysics,  
6                   Chinese Academy of Sciences, No. 19, Beitucheng Western Road, Beijing 100029,

7                                           China. E-mail: eve\_041744@163.com; lfu@mail.iggcas.ac.cn

8       2. China Earthquake Networks Center, No. 5, Sanlihenanhang Avenue, Beijing100036,  
9                                           China.

10       **Abstract**

11           The  $M_s$  8.0 Wenchuan earthquake of May 12, 2008 induces large-amplitude  
12       water level changes at intermediate and far fields (epicentral distance  $>1.5$  fault  
13       rupture length) in Chinese mainland. According to the seismograms, the co-seismic  
14       water level changes are attributed to the dynamic strain induced by the passage of  
15       seismic waves, most probably long period surface waves. Although many hydrologic  
16       changes induced by teleseismic waves have been reported, the mechanisms  
17       responsible for the changes still remain unclear. We invoke Skempton's coefficient  $B$   
18       in this paper to explain those co-seismic water level changes documented in the  
19       intermediate and far fields. Some of those abrupt coseismic water level changes, for  
20       which the variation of the co-seismic water level, Skempton's coefficient  $B$  and the  
21       effective pressure preserve uniformity ( all increase or all decrease ) are found to  
22       favor the consolidation/dilatation induced by the shaking of teleseismic waves. While  
23       the other part of those coseismic water level changes, can be explained with the

24 enhanced permeability caused by fracture clearing or overcoming the capillary  
25 entrapment in porous channels of the aquifer induced by the shaking of teleseismic  
26 waves, and most of those wells lie in basins or in hollows, where the formation is  
27 relatively stable and stiff.

## 28 **Introduction**

29 Various hydrologic responses to earthquakes have been documented (Kayen *et al.*,  
30 2004; Elkhoury *et al.*, 2006; Sil and Freymueller, 2006; Chadha *et al.*, 2008;  
31 Wang and Manga, 2010), many occurred at great distances from the ruptured fault  
32 where static stress changes are relatively small. Hydrologic changes induced by  
33 teleseismic waves have been investigated in several studies of water wells (Roeloffs,  
34 1998; Brodsky *et al.*, 2003; Elkhoury *et al.*, 2006; Geballe *et al.*, 2011). Earthquake  
35 induced water level changes at distant locations were reported after the Denali  
36 earthquake (Brodsky *et al.*, 2003; Kayen *et al.*, 2004; Sil and Freymueller, 2006).  
37 Seismic oscillations, due primarily to surface waves from distant events, occur in  
38 some wells tapping highly transmissive aquifers (Liu *et al.*, 1989; Liu *et al.*, 2006). Sil  
39 and Freymueller (2006) developed an empirical relationship between water level  
40 changes, epicentral distances and earthquake magnitude in the far-field. Chadha *et al.*  
41 (2008) find wells appear to respond to regional strain variations and transient changes  
42 due to distant earthquakes. Liu and Manga (2009) indicate that significant water level  
43 changes can be driven at great distances by moderate-amplitude dynamic  
44 (time-varying) stresses.

45 Several mechanisms have been proposed to explain these co-seismic changes in  
46 water level. Fracture clearing and increased permeability caused by the  
47 earthquake-induced dynamic stress have been widely used to explain most

48 documented far-field water level changes (Brodsky *et al.*, 2003; Elkhoury *et al.*, 2006;  
49 Wang and Chia, 2008; Wang and Manga, 2010). Overcoming the capillary  
50 entrapment in porous channels is hypothesized to be one of the principal pore-scale  
51 mechanisms by which natural permeability is enhanced by the passage of elastic  
52 waves (Beresnev, 2011). Dynamic strain induced by the passage of seismic waves,  
53 most probably long period surface waves might be the cause of water level changes in  
54 the far-field (West *et al.*, 2005; Sil and Jeffrey, 2006; Chadha *et al.*, 2008). Other  
55 proposed, but also unverified mechanisms include pore pressure increases caused by a  
56 mechanism ‘akin to liquefaction’ (Roeloffs, 1998), shaking-induced dilatancy (Bower  
57 and Heaton, 1978), increasing pore pressure through seismically induced growth of  
58 bubbles (Linde *et al.*, 1994), and fracture of an impermeable fault (King *et al.*, 1999).  
59 In addition, Huang (2008) observed the co-seismic water level increase may be  
60 caused by the consolidation induced by the transmission of teleseismic waves in  
61 Fuxin well. Experimental measurements of Liu and Manga (2009) indicate that  
62 permeability changes (either increases or decreases) owing to dynamic stresses are a  
63 reasonable explanation. In general, they find permeability decreases after shaking.

64 In the present study, we use the Skempton’s coefficient  $B$ , the co-seismic water  
65 level and the inferred effective pressure to explain the co-seismic water level changes  
66 in the intermediate and far fields based on datasets from the Wenchuan earthquake in  
67 the Chinese mainland. Using a poroelastic relation between water level and solid tide  
68 (Zhang *et al.*, 2009), we calculate the in-situ Skempton’s coefficient  $B$  both pre and  
69 post earthquake (which are two independent quasistatic processes). From the  
70 research we find: Consolidation/dilatation induced by shaking of teleseismic waves,  
71 may account for the mechanism of those abrupt coseismic water level changes, for

72 which the variations of the co-seismic water level, Skempton's coefficient  $B$  and the  
73 effective pressure preserve uniformity. While, the other part of those coseismic water  
74 level changes, for which the co-seismic water level and the effective pressure change  
75 with inconformity (most of those wells stay in basins with relatively stable and stiff  
76 formations) may be explained with the increased permeability caused by teleseismic  
77 waves, which in turn lead to the redistribution of pore pressure. Compare the  
78 occurrence time of water level changes with the arrival time of surface waves in  
79 several stations, we find the co-seismic water level changes are induced by the long  
80 period surface waves.

## 81 **Selection Principles and Observations**

82 Large numbers of stations with co-seismic water level changes induced by  
83  $M_s$  8.0 Wenchuan earthquake have been collected in the intermediate and far fields  
84 ( $>1.5$  fault-rupture lengths). Most of those water level changes in this area can not be  
85 induced by the change of the static strains, which are extremely tiny ([Zhang and](#)  
86 [Huang, 2011](#)). We selected those co-seismic water level changes with distinct  
87 amplitude (tiny or obscured co-seismic water level changes have been excluded). In  
88 order to calculate the pre- and post- earthquake  $B$  values, water level data in stations  
89 should not be long-time missing or be influenced by other factors, such as pumping or  
90 other disturbances, and the data should be long enough (at least with a 10-day  
91 continuous data before and after the earthquake respectively), so that we can use the  
92 least-square fit to calculate  $B$  ([Appendix](#)). In addition, the oceanic tides has been  
93 known to have an effect several tens of kilometers away from the seashore ([Beaumont](#)  
94 [and Berger, 1975](#)). The deformation caused by ocean tide loading is difficult to  
95 calculate, these tides appear with the same frequencies as the solid earth effects ([Khan](#)

96 and Scherneck, 2003), and the tides are strongly affected by the complicated  
97 topography around the seashore (Walters and Goring, 2001), so we can't simply to  
98 calculate the oceanic tides by theory models. Besides, there are no public software to  
99 calculate the China national offshore ocean tides, so we have to delete those wells (4  
100 wells: Hejiazhuang, Huanghua, Wafangdianloufang and Yongchun) which may be  
101 influenced by the ocean tides seriously. Bearing those rules in mind, we find 11  
102 stations (well a to well k (Figure 1)) can be chosen during the Wenchuan earthquake  
103 (Table 1).

104 Detailed basic information of each well are show in Table 1 , including well  
105 depth, well diameter, aquifer lithology, and geological structure. However, diameter of  
106 well g, h and j can not be found. The detailed borehole columnar diagrams (borehole  
107 columnar diagram of well b, g, h, i, and j can not be found) are not show in this paper,  
108 those information obtained from the borehole columnar diagrams together with the  
109 aquifer lithology are show in Table 1. All the water level recording instruments in  
110 those wells (well a to well k) are digital, they are LN-3A digital water level  
111 instrument (except for Mile well it uses LN-4A digital water level instrument, and  
112 Fuxin well uses the SQ digital water level instrument), with the observation accuracy  
113  $\leq 0.2\%$  F.S. , and the sampling rate of 1/min, the resolution ratio is 1mm. We use the  
114 Mapseis software (Lu *et al.*, 2002) to calculate the tidal strain data (hourly data). In  
115 order to keep in accordance, both the water level and the tidal strain use the hourly  
116 data when calculating the Skempton's coefficient  $B$ .

## 117 **Intermediate and Far Field Analysis**

118 **Assumptions of shear modulus and Poisson's ratio and the calculation of**  
119 **Skempton's coefficient  $B$**

120 Calculations are performed using  $\rho = 1000 \text{ kg / m}^3$ ,  $g = 9.8 \text{ m / s}^2$ , and  $\nu_u = 0.29$   
121 according to equation (5) (Appendix). We suppose the undrained Poisson's ratio  
122  $\nu_u = 0.29$  both pre and after earthquake, and this kind of assumption is always used  
123 to simplify calculation issues of rocks near the crust (Zeng, 1984). In addition, based  
124 on the poroelastic theory, and limited to isotropic conditions, Theo *et al.*(2002) aim to  
125 determine the elastic material constants of the solid matrix with two level of porosities.  
126 As it is not possible to experimentally determine the elastic material constants of the  
127 solid matrix at these levels, a theoretical approach is presented, based on experimental  
128 data taken from literature. They find different porosities lead to different values of  
129 elastic modulus. Their results indicate that the variation extents of Skempton's  
130 coefficient  $B$  and the bulk modulus are much larger than the drained and undrained  
131 poisson's ratios (variation extent of  $B$ : 6.3% ; variation extent of  $K$ : 7.96% variation  
132 extent of  $\nu_u$ : 0.3% ). So we can approximately assume that compared to the  
133 variations of the porous medium modulus (the bulk modulus and Skempton's  
134 coefficient  $B$ ), the change of the undrained poisson's ratio can be neglected before and  
135 after the earthquake.

136 Gassmann (1951) predicted that the effective shear modulus would be  
137 independent of the saturating fluid properties (the shear modulus is a constant) in the  
138 undrained isotropic poroelastic media. As studied by Berryman (1999) and Berryman  
139 and Wang (2001), the theory applies at very low frequencies. At high enough  
140 frequencies (especially in the ultrasonic frequencies), as the numerical simulation of  
141 Berryman and Wang (2001) shows (based on the effective medium theory, and use a  
142 complete set of poroelastic constants for drained Trafalgar shale), with the increase of  
143 Skempton's coefficient  $B$ , the bulk modulus changes by as much as 100% in this  
144 example, whereas the shear modulus changes by less than 10%, and other rock

145 examples also show similar results (Berryman and Wang, 2001). As discussed above,  
146 we can know: It is obvious that the change of shear modulus  $G$  is tiny, and even can  
147 be neglected (both in the drained or undrained cases) as compared with the change of  
148 Skempton's coefficient  $B$ . In this paper we suppose, shear modulus of well aquifer  
149 systems will not change after affected by the seismic waves (the frequencies of  
150 seismic waves are much lower than the ultrasonic frequencies, so the change of the  
151 shear modulus will be neglectable compared to the change in  $B$  value).

152 We apply the  $B$ -calculation method (Appendix) to those well-picked stations.  
153 The pre-and post-earthquake  $B$  values are respectively obtained from May 1, 2008 to  
154 May 11, 2008, and from May 13, 2008 to May 24, 2008 (Figure 2).

### 155 **Undrained Skempton's coefficient $B$ as a function of effective pressure**

156 When the aquifer be consolidated, the effective pressure (effective pressure =  
157 confining pressure - pore pressure) will increase, while a dilation is in accordance to  
158 the decrease of effective pressure. Blocher *et al.* (2009) measured the relationship  
159 between Skempton's coefficient  $B$  and effective pressure based on the laboratory  
160 experiment. The in-situ aquifer of those wells (well a~k) we studied are under  
161 lithostatic pressures for a long time and also be affected by the transmission of  
162 seismic waves for countless times, the situation is much similar to those well bedrocks  
163 be applied on repeated pressure cycles. So the situation will be much similar to the  
164 last several ramps (apply more than once pressure cycles on the rock) rather than the  
165 first ramp (apply the first pressure cycle on the rock, during which a possible  
166 dissolution of gas in the fluid of an incompletely saturated sample happened) in the  
167 experiment of Blocher *et al.* (2009), and the isotropic Skempton's coefficient  $B$  will  
168 increase/decrease with the increase/decrease of effective pressure (when the effective

169 pressure is less than  $\sim 4$  Mpa), while  $B$  will decrease with the increase of effective  
170 pressure (when the effective pressure is larger than  $\sim 4$  Mpa). Although these results  
171 obtained from sandstone, because of the lack of the laboratory experiment study of  
172 those specific rocks, we assume the results can be applied to the bedrock of all those  
173 wells studied in this paper.

174 In order to compare with the experiment results, we have to estimate the  
175 effective pressure of each well. Pore pressure response to gravitational loading is  
176 similar to tectonic loading and can also be treated as a poroelastic problem (Green and  
177 Wang, 1986). Depths of those wells analyzed in this paper are all less than 1km  
178 (Table 1). W-1 well lies in Yanchang basin of Gansu province, Yanchang basin is a  
179 deep basin with Paleozoic sediments (Wu *et al.*, 2010). The “pressure - depth”  
180 relation of well W-1 (Figure 3a) is similar to other wells in the Chinese mainland. So  
181 we assume those results could be applied to these wells we studied (well a  $\sim$  k) since  
182 we lack the “pressure-depth” predictions of these wells. We calculate the effective  
183 pressure of W-1 well (effective pressure approximately equals to lithostatic pressure  
184 minus pore fluid pressure) (Figure 3b), and estimate the range of the effective  
185 pressure of these wells we studied according to the well-depth (Table 1).

186 We calculated the change of pore pressure in each well ( $\Delta P_p = \rho g \Delta h$ ), together  
187 with the range of the effective pressure, the variation trend of Skempton’s coefficient  
188  $B$ , and the  $B$ -effective pressure relation obtained by the experiment of Blocher *et al.*  
189 (2009), we can infer the variation of the effective pressure in each well (Table 2,  
190 Table 3). When the range of the effective pressure lies in 0-3 Mpa (most of the wells),  
191 the increase/decrease of  $B$  accompanied with the increase/decrease of effective



192 pressure. When the range of effective pressure  $>5$  Mpa, the increase/decrease of  $B$   
193 accompanied with the decrease/increase of effective pressure Blocher *et al.* (2009),  
194 only the effective pressure of Jurong well (well f) lies in this range (Table 3).

## 195 **Mechanism analysis**

### 196 **Coseismic water level change induced by consolidation or dilatation**

197 Water level increase/decrease accompanied with the increase/decrease of  
198 Skempton's coefficient  $B$  and the increase/decrease of effective pressure in well a, b,  
199 c, d, g, j, and k (Table 2). To our understanding, suppose the pressure not exceed a  
200 limitation (the fissures not be closed), when the aquifer be consolidated/ dilatated, the  
201 mean fracture width (the porosity and permeability) may decrease/increase with the  
202 increase/decrease of the effective pressure, then the stiff rock matrix that supports the  
203 load could with a higher/lower coupling to the fluid (Nur and Byerlee, 1971), and the  
204 value of  $B$  will increase/decrease. Hence, shaking induced by the transmission of  
205 teleseismic waves may cause consolidation/dilatation of the aquifer, and lead to the  
206 increase/decrease of the water level. Figure 4 shows the relation between the change  
207 of Skempton's coefficient  $B$  and the change of effective pressure (pore pressure/water  
208 level) in well a, b, c, d, g, j, and k . Approximately, it displays a linear relation.

### 209 **Coseismic water level change induced by increased permeability**

210 Water level decrease/increase accompanied with the increase/decrease of  
211 Skempton's coefficient  $B$  and the increases/decrease of effective pressure in well e, h,  
212 and i (Table 3). Fracture clearing (unclogging) and increased permeability may be  
213 used to explain this phenomenon. Since pore-pressure heterogeneity may be the norm

214 in the field, an enhancement of permeability among sites of different pore pressure  
215 may cause pore pressure to spread (Roeloffs, 1998; Brodsky *et al.*, 2003; Wang, 2007;  
216 Wang and Manga, 2010). Pore-pressure of those wells may be higher/lower than other  
217 places before the earthquake, an enhancement of permeability incurred by (for  
218 example) overcoming the capillary entrapment in porous channels induced by the  
219 passage of elastic waves will decrease/increase the pore-pressure in those wells (the  
220 pore-pressure will shift to/shift from other places), and water level will  
221 decrease/increase. Then the effective pressure will increase/decrease accompanied  
222 with the decrease/increase of pore-pressure (water level), so the Skempton's  
223 coefficient  $B$  increase (which indicates the stiff rock matrix could with a higher  
224 coupling to the fluid) in well e, and decrease (which indicates the stiff rock matrix  
225 could with a lower coupling to the fluid) in well h and i (Table 3).

226 The depth of well f (889.18 m) is larger than other wells, and the effective  
227 pressure range of this depth is 8 ~ 10 MPa (Table 3 ). Effective pressure decreases  
228 accompanied with the Skempton's coefficient  $B$  increases in this range (Blocher *et al.*,  
229 2009). So water level increases with the decreases of effective pressure in this well,  
230 and this should be explained with the increased permeability. Pore-pressure of well f  
231 may be lower than other places before the earthquake, an enhancement of  
232 permeability will increase the pore-pressure in this well (the pore-pressure may shift  
233 from other places), and water level will increase. Then the effective pressure will  
234 decrease accompanied with the increase of pore-pressure, so the Skempton's  
235 coefficient  $B$  increase.

236 The local geological structure of each well is important (Table 1), we find that  
237 most of those wells in which permeability increase induced by shaking of teleseismic  
238 waves, stay in basins or in hollows (well e, f, h, i and Fuxin). Due to the mechanical

239 structure, the formation of the basin (or hollow) is relatively solid and stiff, and the  
240 deformation (consolidation or dilatation) will not easily to be incurred, then the  
241 energy of shaking may be inclined to induce the fracture clearing (unclogging) so as  
242 to increase permeability.

### 243 **Examples support far field water level increases induced by consolidation**

244 The spreading of teleseismic waves may cause dilatation of the aquifer medium,  
245 which can broaden the porosities and give birth to new fractures, and the effective  
246 pressure will reduce (in wells: g, j and k, the effective pressure range is 0 ~ 3 MPa)  
247 leading to the decrease of Skempton's coefficient  $B$ . This explanation is similar to the  
248 mechanism of shaking-induced dilatancy (Bower and Heaton, 1978). So it may be  
249 easier to understand water level decreases in the far field induced by the transmission  
250 of teleseismic waves. However, water level increases induced by consolidation in the  
251 far field is not the mainstream view. Since many cases support the theory of the  
252 increased permeability, it is necessary to give some examples which can support far  
253 field water level increases induced by consolidation.

254 Permeability will increase/decrease, which is mostly related to the  
255 increase/decrease of porosity (Xue, 1986). As explained by rock mechanics the same  
256 porosity always corresponding to the same effective pressure (Terzaghi, 1925;  
257 Magara, 1978). From that we can know porosity and permeability are all directly  
258 connected with effective pressure, and they will decrease with the increase of the  
259 effective pressure (Blocher *et al.*, 2009).

260 From the laboratory experiment, Liu and Manga (2009) find that: in general,  
261 permeability decreases after shaking. They measured the evolution of permeability in  
262 fractured sandstone in response to repeated shaking under undrained conditions, and

263 set the frequency and amplitude of the imposed shaking to be representative of those  
264 that cause distant hydrological responses. As they explained: Dynamic strains cause  
265 time varying fluid flow that can redistribute particles within fractures or porespace,  
266 and can allow particles to move away from regions where they hold pore spaces open,  
267 and are expected to accumulate and get trapped at the narrowest constrictions along  
268 flow paths, and hence allow a consolidation (contraction) of the sample. Their result  
269 just supports our mechanism analysis. It implies that teleseismic waves can cause a  
270 consolidation of well aquifer and cause the increase of effective pressure, which is in  
271 accordance with the increase of co-seismic water level changes accompanied with the  
272 increase of Skempton's coefficient  $B$  in wells: a, b, c, d ( effective pressure range 0 ~  
273 3 MPa ).

274 In addition, [Huang \(2008\)](#) find that: the water level increase in Fuxin well  
275 (1409.98 km away from Wenchuan, the well depth is 60.74 m, stiff Granite with a  
276 little basalt is the bedrock and we assume the shear modulus = 60 Gpa) is induced by  
277 the increase of volume strain (consolidation) ([Figure 5a](#)). In the Chinese mainland,  
278 Fuxin is the only well in which there are observations of volume strain and water  
279 level in a specific aquifer medium, and both of them show obvious co-seismic  
280 responses to Wenchuan earthquake. There are clear and obvious effects of tidal strain  
281 and atmospheric pressure in the water level and volume strain, which indicates Fuxin  
282 is a terrific artesian well. This well has not be chosen in the above analysis because  
283 there is an abrupt large-amplitude increase in the water level, which starts from 11  
284 p.m. May 22, 2008 (we can not find any interference of this abrupt increase according  
285 to the daily records of Fuxin station), and we can just use a shorter time period to  
286 calculate the post-earthquake  $B$  value, which may cause a little impact on the precise

287 of  $B$ . The calculation is performed based on the  $M_2$  wave distilled from the water  
288 level and the tidal strain (pre-earthquake: from May 1, 2008 to May 11, 2008,  
289 post-earthquake: from May 13, 2008 to May 22, 2008 (Figure 5b)). (The large-step  
290 abrupt water level increase starts from 09 p.m. May 22, 2008 (Figure 5c), which may  
291 cause large impact on the detrend process and influence the calculation result, so we  
292 discard these data). From Figure 5a, we can see the co-seismic water level increase is  
293 induced by the change of the volume strain, which indicates the well aquifer has been  
294 consolidated. The depth of Fuxin well is 60.74 m, and we can assume the range of the  
295 effective pressure is 0~3Mpa (Table 3), from the change of the pre- and post-  
296 earthquake  $B$  (Figure 5b), we may infer the consolidation may be very extreme,  
297 accompanied with the coseismic water level increase it could cause an extra pressure,  
298 which overcomes the capillary entrapment in porous channels of the aquifer or incurs  
299 a fracture clearing and bring in the increase of the permeability, then water flow in  
300 from other places with a higher pressure, which lead to the decrease of the  
301 Skempton's coefficient  $B$  with the decrease of the effective pressure, and the water  
302 level increases more gradually. Finally with the further enhancement of the  
303 permeability (increase of the porosity), a permanent deformation could be induced, so  
304 there is an abrupt increase in the water level in 22 May, and remain in a relatively  
305 high level for several months(Figure 5c). From the picture we can see it may be in a  
306 drained condition after the abrupt large-amplitude water level increase, because the  
307 water level fluctuates irregularly.

308 So we argue that water level increase induced by the consolidation incurred by  
309 transmission of teleseismic waves is reasonable, and in a specific geology condition,  
310 a consolidation with large enough energy may also lead to an enhanced permeability  
311 by fracture clearing or by overcoming the capillary entrapment in porous channels.

312 **Wellbore storage effects**

313 Tidal phase lags are caused by wellbore storage. “Wellbore storage” is the term  
314 used to describe a lag of piezometer water level behind aquifer pressure resulting  
315 from the need for water to flow into the borehole in order to equilibrate water level  
316 with aquifer pressure. Wellbore storage effects increase (phase lags increase) as the  
317 transmissivity (and permeability) of the formation decreases (Roeloffs, 1996; Doan *et*  
318 *al.*, 2006).

319 Most of those wells can record clear tidal strain and atmospheric pressure, and  
320 according to the <China earthquake monitoring records series> (which is written by  
321 different Subordinate units (earthquake administration of each provinces and different  
322 institutions) of China Earthquake Administration, and published in Beijing in  
323 different years by Seismological Press (in Chinese)) they are well confined. From  
324 [Table 1](#) we can see the phase difference of water level and tidal strain of most wells  
325 are 0, which mean good correlations between the water levels and the tidal strains,  
326 and those wells are well confined and under the undrained condition. Because we use  
327 the hourly data, we can not identify the phase difference when it is less than 1 hour,  
328 and we just neglected the wellbore storage effects in those wells. Before and after the  
329 earthquake, if phase lags remain the same, it indicates the permeability of the well  
330 aquifer keeps the same or just changes a little (the phase difference may be less than 1  
331 hour). Phase lags  $\geq 1$  hour in well: b, c, e, and Fuxin, and most of them are small,  
332 except well b, which may be semi-confined. Thus, the validity of the calculated  $B$   
333 values in well b may be a little questionable. The phase lag of Fuxin well decreases  
334 after the earthquake ( $L_1=2$  hours,  $L_2=1$  hour), which indicates the permeability  
335 increases after the shaking of the earthquake, this is in accordance with the mechanism  
336 analysis of the co-seismic water level increase in Fuxin well.

## 337 **Discussion**

### 338 **The variation of porosity**

339 [Figure 3c](#) shows, in general, the porosity decreases with the increase of depth,  
340 however, when reach 3000m the effective pressure turns much larger (approximately  
341 equals to 35 Mpa) than that in the depth of those wells (well a ~ k), the porosity still  
342 persists relatively large, and changes with different depth. From [Table 2](#) we can see,  
343 the variation of effective pressure of well a, b, c, d, g, j and k is less than 0.01Mpa,  
344 and from [Figure 3b](#) we know, variation of 0.01Mpa in effective pressure  
345 approximately equals to variation of 1 meter in depth, as [Figure 3c](#) shows, the  
346 variation of porosity is tiny during variation of 1 meter in depth. So this variation  
347 extent of effective pressure is hard to induce permanent deformation of porosity.  
348 However, in reality, the change of porosity may also connected with the formation  
349 and the state of the rock matrix.

350 Furthermore, phase lags of well a, b, c, d, g, j and k keep constant before and  
351 after the earthquake (change less than 1 hour) ([Table \(1\)](#)), so we can infer, the  
352 porosity (permeability) change little after the earthquake. Because the phase lags  
353 increase/decrease (wellbore storage effects increase/decrease) as the permeability  
354 (porosity) of the formation decreases/increase ([Roeloffs, 1996; Doan et al., 2006](#)).

355 So we can infer, the porosity of well a, b, c, d, g, j and k can persist despite being  
356 reduced/enlarged due to the consolidation/dilatation induced by the passage of  
357 teleseismic waves of  $M_s$  8.0 Wenchuan earthquake.

### 358 **Uncertainty of $B$ coefficient**

359 In order to study the uncertainty of  $B$  coefficient (error related to the

360 determination of  $B$  coefficient), we use Jurong well to show the variation of  $B$  during  
361 a relatively long – time span (50 days before and after the Wenchuan earthquake)  
362 (Figure 6). Skempton’s coefficient  $B$  will change with the change of time. Because we  
363 use the least square fit to calculate  $B$ , the value may be a little different when we use  
364 different length of data , but the change tendency (increase or decrease of  $B$ ) before  
365 and after the earthquake will be constant. Furthermore, we can see the  $B$  value of  
366 Jurong well recover to its initial value after about 30 days (Figure 6).

367 So, compared with the uncertainty in  $B$  value, variation of  $B$  due to the  
368 earthquake is significant. The continuous of  $B$  will be influenced by lots of factors,  
369 such as power off, aftershocks, and so on, so  $B$ -value series at large time scale is not  
370 easy to obtain for each well.

### 371 **Recovery of Water level**

372 The recovery time of the water level is obscure, because most of those water  
373 level will not recover to the same height as the pre-earthquake level during a  
374 relatively short time span. So we should use much longer data to analyze it, and  
375 should discard all those influences: such as aftershocks, atmospheric pressure ( not all  
376 those wells have the records of atmospheric pressure ) , tidal strain, pumping, power  
377 off, thunder and so on, which needs lots of work, and we may study about it in future.  
378 In addition, we haven’t find any relation between water level changes and epicentral  
379 distances in those wells studied in this paper, it is possible to investigate much more  
380 wells later, to study about the relations.

### 381 **The variation value of effective pressure**

382 We calculated the change of pore pressure ( $\Delta p_p = \rho g \Delta h$ ), and we can use the



383 critical state to help us to analyze the variation value of effective pressure in each  
384 well.

385 When the aquifer be consolidated/dilated, in the critical state, the pore pressure  
386 keeps constant, the confining pressure increase /decrease, then the effective pressure  
387 increase/decrease, and at last transfer into the increase/decrease of pore pressure  
388 (water level increase/decrease), and the system comes into an equilibrium state. So the  
389 change of pore pressure can be attributed to the change of the effective pressure.

390 When the permeability increase, in the critical state, the confining pressure keeps  
391 constant, the pore pressure (water level) increase (the well in a relatively low pressure  
392 region before the earthquake) /decrease (the well in a relatively high pressure region  
393 before the earthquake), then the effective pressure decrease/increase, so the change of  
394 the effective pressure can be attributed to the change of pore pressure.

395 However , the variation value of the effective pressure of each well may be  
396 different from the value we calculate, because the critical state is an assumption ideal  
397 state, and the transfer of stress may also relate with the formation and state of the  
398 aquifer.

### 399 **Compare with seismograms**

400 There are 48 national stations recording the seismograms (event waveforms) in  
401 the Chinese mainland (we can not obtain the regional seismograms because of the  
402 authority limitation), however most of those stations are not in the same place with  
403 stations which have the records of water level changes. Those stations (well a to k)  
404 analyzed in our paper have no records of seismograms. After comparison, generally  
405 we may use the seismograms of 4 national stations to analyze the corresponding water

406 level observations (Figure 7), which are near those national stations (the distances  
407 between the water level wells and the national seismogram stations are approximately  
408 less than 100km). We use the seismogram of Sheng yang (SNY) national station to  
409 analyze Fuxin well (there are about 102.81 km between them), while Taiyuan (TIY)  
410 national station is corresponding to well e (there are about 40.903 km between them);  
411 Lanzhou (LZH) station is corresponding to well g (there are about 19.82 km between  
412 them); and Hefei (HEF) station is corresponding to well k (there are about 91.57 km  
413 between them). In addition, the geology conditions are very similar (the main bed  
414 rock of Fuxin well and Shengyang station are both granite; Well e is in the east of  
415 Taiyuan basin, bed rock of well e and Taiyuan station are both limestone; Well k is in  
416 Chuhe river major dislocation and Hefei--Dongguan fracture intersection; bed rock of  
417 well g and Lanzhou station are both sandstone).

418 However, because the Z-component seismogram of TIY national station is  
419 deficient, we have to give up the analysis of Z component in TIY station. The  
420 waveforms in LZH station is also deficient, there may be some disturbances (Figure  
421 7). There are only hourly water level data in Fuxin well (minute data observation  
422 strats from 2009), so we can not use that to do precise comparison (in minute) with  
423 the seismogram. In general, we can only use well e and well k to do the comparisons  
424 between the timing of steps in water level changes and the arrival time of waves in  
425 seismograms.

426 From the occurrence time of water level changes and the arrival time of surface  
427 waves of well e and well k (Table 4), we find the co-seismic water level changes are

428 attributed to the passage of surface waves in the two wells. From that, we may infer:  
429 in other wells the co-seismic water level changes are attributed to the dynamic strain  
430 induced by the passage of teleseismic waves, most probably surface waves, which  
431 have relatively larger amplitude of oscillation, corresponding to relatively larger  
432 energy. The similar conclusion has been proposed by [Sil and Jeffrey \(2006\)](#), [West \*et al.\* \(2005\)](#), and [Chadha \*et al.\* \(2008\)](#).

434         Since well g and well k are all induced by the dilatations incurred by teleseismic  
435 waves, we can do some comparisons between them. From the seismograms we can  
436 see, the velocity amplitude of LZH (near well g) is much larger than that of HEF (near  
437 well k), so the energy of the teleseismic waves is much larger in well g than in well k  
438 (energy is in direct proportion to the square of the amplitude of oscillation). However,  
439 the amplitude of the co-seismic water level changes are not only related to the energy,  
440 but also connected with the different local geology conditions, such as the extent of  
441 the coupling between the solid matrix and the fluid (Skempton's coefficient  $B$  ( $B$   
442 value of well k is larger than that of well g)), so the amplitude of the coseismic water  
443 level change of well k is larger than that of well g.

444         Because of the low temporal resolution of the water level data, further analysis of  
445 the steps could not be made. Co-seismic water level changes occurred in the 2 wells  
446 (well e and well k) during the passage of surface waves. More precise estimation of  
447 the timing of the step could not be made because of the low temporal resolution of the  
448 water level data. Obviously, there are geographic position difference between the  
449 observation of seismograms and water levels, and there are also some errors on the

450 manual amplitude readings, both of which could cause some influence on the analysis.

451 From the geological structures, we find that most of those wells in which  
452 permeability increase induced by shaking of teleseismic waves, stay in basins or in  
453 hollows (well e, f, h, i and Fuxin), which may be attributed to the relatively stiff  
454 formation of those basins or hollows due to the mechanical structure. According to the  
455 the diverse and very complicated geology conditions, we may focus on 1—2 wells  
456 (which record both the water level and the seismogram), to do much more deeply  
457 analysis in future, so as to reveal the mechanism more deeply and clearly.

## 458 **Conclusion**

459 Together with the variation of Skempton's coefficient  $B$ , the change of pore  
460 pressure and the inferred variation of effective pressure in each well, we can infer the  
461 mechanism of the co-seismic water level changes. From the study we can conclude:  
462 consolidation/dilatation induced by shaking of teleseismic waves, may account for the  
463 mechanism of those abrupt coseismic water level changes, for which the variation  
464 tendency of the co-seismic water level, Skempton's coefficient  $B$  and the effective  
465 pressure keep the same (all increase or all decrease). While, fracture clearing and  
466 increased permeability may be used to explain the other part of those coseismic water  
467 level changes, for which the co-seismic water level, and the effective pressure change  
468 with inconformity, and most of those wells stay in basins with relatively stable and  
469 stiff formations. Compared with the seismograms, the co-seismic water level changes  
470 are attributed to the dynamic strain induced by the passage of seismic waves, most  
471 probably long period surface waves. Our analysis is not conflict with any of those  
472 existing theories. Although those water level changes happened in the intermediate

473 and far fields, most of those water levels present abrupt and obvious co-seismic  
474 changes owing to the huge energy of  $M_s$  8.0 Wenchuan earthquake.

475 From the analysis of Fuxin well, we can see a consolidation with large enough  
476 energy may overcome the capillary entrapment in porous channels or clear the  
477 fractures, and incur an enhanced permeability. So as discussed by [Liu and Manga](#)  
478 (2009), permeability changes (either increases or decreases) owing to dynamic  
479 stresses are reasonable explanations for earthquake-induced hydrologic responses.  
480 The mechanisms analyzed in this paper are similar to the experiment results of [Liu](#)  
481 [and Manga](#) (2009), and our in-situ analysis may complement the limitation of the  
482 initial condition of their laboratory experiments.

483 In reality, the shear modulus  $G$  and the undrained Poisson's ratio  $\nu_u$  would  
484 change slightly after the shaking of seismic waves, and the discussed "undrained"  
485 condition can hardly last for a long time, as long as the fluid flow exists, the  
486 undrained condition will disrupt and be replaced by the drained condition soon. We  
487 assume the results get from sandstone can be applied to all those bedrocks in those  
488 wells ([Figure 3](#)), however this is not very precise. As described by [Wang](#) (1993)  
489 nonlinear compaction effects can be significant and they are not incorporated in the  
490 linear theory presented here, because the well aquifers are under lithostatic pressures  
491 for a long time and withstand large numbers of seismic shaking, the irreversible  
492 deformations and the nonlinear effects have been minimized (In the laboratory  
493 experiment, in order to reduce the irreversible deformation and to minimize the  
494 nonlinear effects, repeated pressure cycles are always applied on rock samples as  
495 preconditions ([Blocher et al., 2009](#))). Discard all those ideal assumptions, things may  
496 be different.

## 497 **Data and Resources**

498 Data used in this paper were collected using a classified network (Groundwater  
499 Monitoring Network, GMN) of the China Earthquake Networks Center and cannot be  
500 released to the public. We use the Mapeis software (Lu *et al.*, 2002) to calculate the  
501 tidal strain data.

502 **Acknowledgements.** We thank professor Emily Brodsky and postdoctor  
503 Jinlai Hao for discussion and help on this paper. This research was supported by the  
504 Natural Science Foundation of China (Grant No. 40925013 and 41040036). We  
505 gratefully appreciate the valuable suggestions proposed by the anonymous reviewers.

## 506 **Reference**

- 507 Brodsky, E., E. Roeloffs, D. Woodcock, I. Gall, and M. Manga (2003). A mechanism  
508 for sustained groundwater pressure changes induced by distant earthquake, *J.*  
509 *Geophys. Res.* **108(B8)**, 2390.
- 510 Beresnev, I., W. Gaul, and R. D. Vigil (2011). Direct pore-level observation of  
511 permeability increase in two-phase flow by shaking, *Geophys. Res. Lett.* **38**,  
512 L20302.
- 513 Blocher G., G. Zimmermann and H. Milsch (2009). Impact of poroelastic response of  
514 sandstone on geothermal power production, *Pure appl. geophys.* **166**,  
515 1107–1123.
- 516 Bower, D. R., and K. C. Heaton (1978). Response of an aquifer near Ottawa to tidal  
517 forcing and the Alaskan earthquake of 1964, *Can. J. Earth Sci.* **15**, 331–340.
- 518 Berryman, J. G., and H. F. Wang (2001). Dispersion in poroelastic systems, *Phys. Rev.*  
519 *E* **64**, 011303.
- 520 Berryman, J. G. (1999). Origin of Gassmann's equations, *Geophysics* **64**, 1627–1629.

- 521 Beaumont, C. and J. Berger (1975). An analysis of tidal strain observations from the  
522 United States of America: I. The laterally homogeneous tide, *Bull. Seismol. Soc.*  
523 *Am.* **65**, 1613–1629.
- 524 Chadha, R. K., C. Singh, and M. Shekar (2008). Transient changes in well-water level  
525 in bore wells in western India due to the 2004 Mw 9.3 Sumatra Earthquake,  
526 *Bull. Seismol. Soc. Am.* **98**, 2553–2558.
- 527 Chadha, R. K., H. J. Kuempel and M. Shekar (2008). Reservoir triggered seismicity  
528 (RTS) and well water level response in the Koyna-Warna region, India.  
529 *Tectonophysics* **456**, 94–102.
- 530 Doan, M. L., E. E. Brodsky, R. Prioul and C. Signer (2006). Tidal analysis of  
531 borehole pressure-A tutorial, *Schlumberger Research report*, P35.
- 532 Elkhoury, J. E., E. E. Brodsky and D. C. Agnew (2006). Seismic waves increase  
533 permeability, *Nature* **411**, 1135–1138.
- 534 Green, D. H. and H. F. Wang (1986). Fluid pressure response to undrained  
535 compression in saturated sedimentary rock, *Geophysics* **51(4)**, 948–956.
- 536 Geballe, Z. M., C.-Y. Wang, and M. Manga (2011). A permeability-change model for  
537 water-level changes triggered by teleseismic waves, *Geofluids* **11**, 302–308.
- 538 Gassmann, F. (1951). Über die elastizität poröser medien, *Vierteljahrsschrift der*  
539 *Naturforschenden Gesellschaft in Zürich*, **96**, 1–23.
- 540 Huang, F.-Q. (2008). *Response of Wells in Groundwater Monitoring Network in*  
541 *Chinese Mainland to Distant Large Earthquakes*, [Ph.D Dissertation] Institute  
542 of Geophysics, China Earthquake Administration, Beijing, pp. 47, (in Chinese).
- 543 Kan, S. A., and H. G. Scherneck (2003). The M2 ocean tide loading wave in Alaska:

544 vertical and horizontal displacements, modelled and observed, *J. Geodesy* **77**,  
545 117–127.

546 Kayen, R. E., E. Thompson, D. Minasian, R. E. S. Moss, B. D. Collins, N. Sitar, D.  
547 Dreger, G. A. Carver (2004). Geotechnical reconnaissance of the 2002 Denali  
548 Fault, Alaska, Earthquake. *Earthq. Spectra* **20**, 639–667.

549 King, C.-Y., S. Azuma, G. Igarashi, M. Ohno, H. Saito, and H. Wakita (1999).  
550 Earthquake-related water-level changes at 16 closely clustered wells in Tono,  
551 central Japan, *J. Geophys. Res.* **104**, 13,073–13,082.

552 Linde, A. T., I. S. Sacks, M. J. S. Johnston, D. P. Hill, and R. G. Bilham (1994).  
553 Increased pressure from rising bubbles as a mechanism for remotely triggered  
554 seismicity, *Nature* **371**, 408–410.

555 Liu, W. Q., M. Manga (2009). Changes in permeability caused by dynamic stresses in  
556 fractured sandstone, *Geophys. Res. Lett.* **36**, L20307.

557 Liu, C., M. W. Huang, and Y. B. Tsai (2006). Water level fluctuations induced by  
558 ground motions of local and teleseismic earthquakes at two wells in Hualien,  
559 eastern Taiwan, *TAO* **17**, 371–389.

560 Liu, L.B., E. Roeloffs, and X. Y. Zheng (1989). Seismically induced water level  
561 fluctuations in the Wali Well, Beijing, China, *J. Geophys. Res.* **94**, 9453–9462.

562 Lu, Y. Z., S. L. Li, Z. H. Deng, H. W. Pan, S. Che, and Y. L. Li (2002). *Seismology*  
563 *Analysis and Prediction System Based on GIS (Mapseis Software)*, Chengdu  
564 Map Press, Chengdu, China, 232.

565 Magara, K. (1978). Compaction and fluid migration, *Practical petroleum geology*.



566 Amsterdam: Elsevier Scientific Publishing Company, 1–319.

567 Nur, A., and J. Byerlee (1971). An exact effective stress law for elastic deformation of  
568 rocks with fluids, *J. Geophys. Res.* **76**, 6414–6419.

569 Rice, J. R., and M. P. Cleary (1976). Some basic stress diffusion solutions for fluid-  
570 saturated elastic porous media with compressible constituents, *Rev. Geophys.* **14**,  
571 227–241.

572 Roeloffs, E. A. (1996). Poroelastic techniques in the study of earthquakes-related  
573 hydrologic phenomena, *Adv. Geophys.* **37**, 135–195.

574 Roeloffs, E. A. (1998). Persistent water level changes in a well near Parkfield,  
575 California, due to local and distant earthquakes, *J. Geophys. Res.* **103**, 869–889.

576 Sil, S. (2006). Response of Alaskan wells to near and distant large earthquakes,  
577 Master’s Thesis, University of Alaska Fairbanks, pp. 8–11.

578 Sil, S. and J. T. Freymueller (2006). Well water level changes in Fairbanks, Alaska,  
579 due to the great Sumatra-Andaman earthquake, *Earth Planets Space* **58**,  
580 181–184.

581 Terzaghi, K. (1925). Principles in soil mechanics, III. Determination of the  
582 permeability of clay, *Engineering News Record.* **95**, 832–836.

583 Theo, H. S., M. H. Jacques, and C. C. Stephen (2002). Estimation of the poroelastic  
584 parameters of cortical bone, *J. Biomech.* **35**, 829–835.

585 Wang, H. F. (2000). *Theory of linear poroelasticity with application to geomechanics*  
586 *and hydrogeology*. Princeton University Press, Princeton, pp. 5–6.

587 Wang, H. F. (1993). Quasi-static poroelastic parameters in rock and their geophysical  
588 applications, *PAGEOPH* **141**, 269–286.

589 Wang, C.-Y. (2007). Liquefaction beyond the near field, *Seismol. Res. Lett.* **78**,  
590 512–517.

591 Wang, C.-Y., and M. Manga (2010). *Earthquakes and Water, Series: Lecture Notes in*  
592 *Earth Sciences*. Springer Press, Berlin, pp. 18–24.

593 Wang, C.-Y., and Y. Chia (2008). Mechanism of water level changes during  
594 earthquakes: Near field versus intermediate field, *Geophys. Res. Lett.* **35**,  
595 L12402.

596 Walters, R. A. and D. G. Goring (2001). Ocean tides around New Zealand, *New. Zeal.*  
597 *J. Mar. Fresh.* **35**, 567–579.

598 Wu, H. Z., L. Y. Fu and H. K. Ge (2010). Quantitative analysis of basin-scale  
599 heterogeneities using sonic-log data in the Yanchang Basin, *J. Geophys. Eng.* **7**,  
600 41–50.

601 West, M., J. Sanchez, and S. McNutt (2005). Periodically-triggered seismicity at Mt.  
602 Wrangell volcano following the Sumatr earthquake, *Science*, **308**,1144–1146.

603 Xue, Y.-Q. (1986). *Groundwater dynamics*. Geology Press, Beijing, pp. 16, (in  
604 Chinese).

605 Zhang, Y., F. Q. Huang, and G. J. Lai (2009). Research on Skempton’s coefficient  $B$   
606 based on the observation of groundwater of Changping station, *Earthq. Sci.* **22**,  
607 631–638.

608 Zhang, Y., and F. Q. Huang (2011). Mechanism of Different Coseismic Water-Level  
609 Changes in Wells with Similar Epicentral Distances of Intermediate Field, *Bull.*  
610 *Seismol. Soc. Am.* **101**, 1531–1541.

611 Zeng, R. S. (1984). *Solid Geophysics Introduction*, Press of Science, Beijing, pp. 9,  
612 (in Chinese).

613 Zhao L. F., X. B. Xie, W. M. Wang, and Z. X. Yao (2008). Regional Seismic  
614 Characteristics of the 9 October 2006 North Korean Nuclear Test, *Bull. Seismol.*  
615 *Soc. Am.* **98**, 2571–2589.

616

### 617 **Appendix: An approach to Skempton's coefficient $B$ based on the** 618 **poroelastic theory**

619 Skempton's coefficient  $B$  is a significant pore-fluid parameter in poroelastic  
620 theory. A poroelastic material consists of an elastic matrix containing interconnected  
621 fluid saturated pores. Fluid saturated crust behaves as a poroelastic material to a good  
622 degree of approximation.

623 [Rice and Cleary \(1976\)](#) summarized the following equations for a linearly elastic  
624 isotropic porous medium (they are the building blocks of the poroelastic theory):

$$625 \quad 2G\varepsilon_{ij} = \sigma_{ij} - \frac{\nu}{1+\nu} \sigma_{kk} \delta_{ij} + \frac{3(\nu_u - \nu)}{B(1+\nu)(1+\nu_u)} p \delta_{ij}, \quad (1)$$

$$626 \quad m - m_0 = \frac{3\rho(\nu_u - \nu)(\sigma_{kk} + 3p/B)}{2GB(1+\nu)(1+\nu_u)}. \quad (2)$$

627 Here  $m - m_0$  is the change of the fluid mass,  $\varepsilon_{ij}$  is the strain tensor,  $\sigma_{ij}$  is the stress  
628 tensor,  $\delta_{ij}$  is the Kronecker delta function,  $G$  is the shear modulus,  $\rho$  is the  
629 density of the fluid,  $B$  is the Skempton's coefficient,  $p$  is the pore pressure,  $\nu$  is  
630 the Poisson's ratio, and  $\nu_u$  is the "undrained" Poisson's ratio. [Rice and Cleary \(1976\)](#)  
631 describe equation (1) as a stress balance equation and equation (2) as a mass balance  
632 equation.

633 For the undrained condition, the poroelastic effect on the crust can be obtained  
634 by putting  $m - m_0 = 0$  in equation (2) to obtain

$$635 \quad p = -B\sigma_{kk} / 3 \quad \text{or} \quad \Delta p = -B\Delta\sigma_{kk} / 3. \quad (3)$$

636 Equation (3) indicates that, in the undrained condition, the change in fluid pressure  
637 ( $\Delta p$ ) is proportional to the change in mean stress ( $\Delta\sigma_{kk} / 3$ ). This is the mechanism of  
638 water level changes for poroelastic material. ( $p = \rho gh$ , where  $h$  is the water column  
639 height,  $g$  is the acceleration due to gravity and  $\rho$  is the density of water).

640 According to equation (3), Skempton's coefficient  $B$  can be qualitatively defined:  
641 In the undrained condition,  $B$  is the ratio of the induced pore pressure divided by the  
642 change in mean stress (Wang, 2000).  $B$  governs the magnitude of water-level changes  
643 due to an applied stress because pore pressure is directly proportional to water level.  
644 The value of  $B$  is always between 0 and 1. When  $B$  is 1, the applied stress is  
645 completely transferred into changing pore pressure. When  $B$  equals 0, there is no  
646 change in pore pressure after applying the stress. Thus a low value of  $B$  indicates the  
647 stiff rock matrix that supports the load with low coupling to the fluid (Nur and  
648 Byerlee, 1971). Laboratory studies indicate the value of  $B$  depends upon the fluid-  
649 saturated pore volume of the sample (Wang, 2000).

650 Equation (3) can be expressed in terms of tidal strain as well (Roeloffs, 1996):

$$651 \quad \Delta h = -\frac{2GB(1 + \nu_u)}{3\rho g(1 - 2\nu_u)} \Delta \varepsilon_t. \quad (4)$$

652 Equation (4) shows that water level changes proportionally in a poroelastic material  
653 under the influence of tidal strain ( $\varepsilon_t$ ). Here,  $\Delta h$  is the change in height of water  
654 level, and  $\Delta \varepsilon_t$  is the corresponding tidal strain change (Sil, 2006).

655 From equation (4) we obtain:

656 
$$B = -\frac{3\rho g(1-2\nu_u)}{2G(1+\nu_u)} \frac{\Delta h}{\Delta \varepsilon_t}. \quad (5)$$

657 With equation (5), we obtain the value of  $B$  with water level and tidal strain. However,  
 658 the calculation must be on the strict premise of the undrained condition (the good  
 659 correlation between the water level and the tidal strain) and should not be influenced  
 660 by the other factors.

661 For the effect of the solid tide on the crust, when the wavelength of the tidal  
 662 strain is much larger than the size of the aquifer, we can suppose the aquifer system is  
 663 undrained (Huang, 2008). So we can suppose the effect of the  $M_2$  wave in the crust  
 664 can meet the undrained condition (Zhang *et al.*, 2009). In addition, those wells can  
 665 record clear tidal strains and thus, because we calculate the phase lags between the  
 666 water levels and the tidal strains are small, the wells can readily meet the undrained  
 667 condition. In the  $M_2$ - wave frequency domain, the water level and the tidal strain  
 668 show a good correlation; Furthermore, the  $M_2$  wave is hardly influenced by  
 669 atmospheric pressure. We therefore distill the frequency domain of the  $M_2$  wave  
 670 from the water level and the tidal strain by using band-pass filter (the frequency of the  
 671  $M_2$  wave is  $2.23636 \times 10^{-5} \text{ HZ}$  ) to calculate the Skempton's coefficient  $B$ . By  
 672 converting the frequency domain of the  $M_2$  waves (obtained from the water level and  
 673 the tidal strain), by inverse fast Fourier transform and adjusting their phases (using the  
 674 least-square fit and putting the results into equation (5)), we can finally derive  $B$ .  
 675 (More details of the method are explained in Zhang *et al.*, 2009). All the Water-level  
 676 observations come from the sensor of water level, while tidal strain data are calculated  
 677 via Mapseis software (see Data and Resources section). One thing needs to be  
 678 clarified: We haven't applied the static equations directly to relate pore pressure

679 changes to seismic waves. We use those static equations for the impact of the tidal  
680 strain on the aquifer medium before and after the Wenchuan earthquake, so as to  
681 obtain the pre- and post- earthquake Skempton's coefficient  $B$  (those two periods can  
682 be recognized as two independent quasi-static processes), so the poroelastic static  
683 equations can be applied.

Table 1. Basic information of well a ~ k.

Station	Epicentral Distance /km	$\Delta h/m$	Pre/Post-Earthquake $B$	Major Aquifer Lithology	$G^*/Gpa$	Phase Lag/hour	Well Diameter /mm	Well Depth/m	Range of $P_{eff}/MPa$	Geological Structure
(a) Xiaxian	465.9465	0.106	0.0123/0.0149	Biotite plagioclase gneiss and mild clay	40	L1=L2=0	559	170.5	0~3	north part of Zhongtiao mountain fault
(b) Mile	726.4589	0.579	0.0872/0.1103	Limestone	20	L1=L2=-6	127	614.4	3~5	Mile—Shizong fault
(c) Qinxianmanshui	983.8517	0.172	0.0557/0.0653	Three of Triassic sandstone	8	L1=L2=-2	134	240.05	0~3	Guocun basin, uplift of Taihang mountain fault block
(d) Xiaoyi	1062.0768	0.398	0.1493/0.186	P2 Sandstone	8	L1=L2=0	150	502.93	0~3	Jiaocheng fault
(e) Qixian	1152.6034	0.831	0.0906/0.0153	Limestone and shale (the Tertiary and Quaternary period loess and gravel)	20	L1=0 L2=-3	146	442.19	0~3	east part of Taiyuan basin
(f) Jurong	1750.2357	0.263	0.0472/0.0519	K2 Silicified sandstone and conglomerate	8	L1=L2=0	219	889.18	8~10	west of Maoshan mountain fault, near the top of the uplift of the buried hill of Jurong hollow
(g) Haiyunganyanchi	606.402	-0.036	0.0407/0.0395	Q sandstone and conglomerate	8	L1=L2=0		306.73	0~3	west and south of Huashan mountain fault
(h) Guyuanzhenqi	638.7904	-0.026	0.0026/0.0047	Mediate and fine sand	8	L1=L2=0		255.74	0~3	compresso-shear basin, in the east and north part of Haiyuan fault
(i) Kaiyuan	805.4263	-0.155	0.0724/0.077	Triassic Falang formation limestone	20	L1=L2=0	273	224	0~3	south of Xiaojiang fault, east of arc structure top, in the northern part of the basin
(j) Meizhou	1345.951	-0.075	0.0873/0.0823	Quartzite	20	L1=L2=0		338.86	0~3	Heyuan—Shaowu and Chaoan—Meixian fracture intersection
(k) Chaohu	1587.6013	-0.455	0.091/0.0798	The Devonian quartz and limestone	20	L1=L2=0	168	331	0~3	East side of the Tanlu fault, Chuhe river major dislocation and Hefei—Dongguan fracture intersection.
Fuxin	1409.9764	0.121	0.5761/0.5145	Granite, basalt, andesite and clip tuff breccia	60	L1=-2 L2=-1		60.74	0~3	west and north of Fuxin fault basin

Epicentral Distances, Water Level Changes, Pre- and Post- Earthquake  $B$  Values, Major Lithology of Aquifers, Shear Modulus, Phase Lags, Well Diameters, Well Depths, Ranges of Effective Pressure and Geological Structures of those well-picked stations. L1 and L2 represent the pre- and post- earthquake phase lags (the lag of piezometer water level behind the tidal strain induced aquifer pressure) separately.

Shear modulus  $G^*$  see Yan Zhang and Fuqiong Huang (2011).



**Table 2.** Coseismic water level changes induced by consolidation or dilatation incurred by shaking of teleseismic waves.

Station	$\Delta h/m$	$\Delta B$	$\Delta P_p/MPa$	$\Delta P_{eff}/MPa$	Well Depth/m	Range of $P_{eff}/MPa$
(a) Xiaxian	0.106	<b>0.0026</b>	0.0010	<b>0.001</b>	170.5	0~3
(b) Mile	0.579	<b>0.0231</b>	0.0057	<b>0.0057</b>	614.4	3~5
(c) Qinxianmanshui	0.172	<b>0.0096</b>	0.0017	<b>0.0017</b>	240.05	0~3
(d) Xiaoyi	0.398	<b>0.0367</b>	0.0039	<b>0.0039</b>	520.93	0~3
(g) Haiyuanganyanchi	-0.036	<b>-0.001</b>	-0.0004	<b>-0.0004</b>	306.73	0~3
(j) Meizhou	-0.075	<b>-0.005</b>	-0.0007	<b>-0.0007</b>	338.86	0~3
(k) Chaohu	-0.455	<b>-0.011</b>	-0.0045	<b>-0.0045</b>	331	0~3

Water Level Changes, Changes of  $B$  Value, Calculated Changes of Pore-Pressure  $\Delta P_p$ , Inferred Changes of Effective Pressure  $\Delta P_{eff}$ , Well Depths and Ranges of Effective Pressure of those wells.

**Table 3.** Coseismic water level changes induced by increased permeability.

Station	$\Delta h/m$	$\Delta B$	$\Delta P_p/MPa$	$\Delta P_{eff}/MPa$	Well Depth/m	Range of $P_{eff}/MPa$
(e) Qixian	0.831	<b>-0.075</b>	0.0081	<b>-0.0081</b>	422.19	0~3
(f) Jurong	0.263	<b>0.0047</b>	0.0026	<b>-0.0026</b>	889.18	8~10
(h) Guyuanzhenqi	-0.026	<b>0.0021</b>	-0.0003	<b>0.0003</b>	255.74	0~3
(i) Kaiyuan	-0.155	<b>0.0046</b>	-0.0015	<b>0.0015</b>	224	0~3
Fuxin	0.121	<b>-0.0616</b>	0.0012	<b>-0.0012</b>	60.74	0~3

Water Level Changes, Changes of  $B$  Value, Calculated Changes of Pore-Pressure  $\Delta P_p$ , Inferred Changes of Effective Pressure  $\Delta P_{eff}$ , Well Depths and Ranges of Effective Pressure of those wells.

**Table 4.** Occurrence time of water level changes and arrival time of surface waves.

Well <sub>(water level)</sub> / Station <sub>(seismogram)</sub>	Occurrence time of water level change/min	Arrival time of surface wave/s	Seismogram quality
(g) Haiyuanganyanchi / LZH	14:27:00, May 12, 2008	14:28:24.5, May 12, 2008	deficient
(e) Qixian / TIY	14:35:00, May 12, 2008	14:30:59.5, May 12, 2008	(z component) deficient
(k) Chaohu / HEF	14:32:00, May 12, 2008	14:31:59.5, May 12, 2008	good
Fuxin (only hour data) / SNY	14:??, May 12, 2008	14:36:19.5, May 12, 2008	good

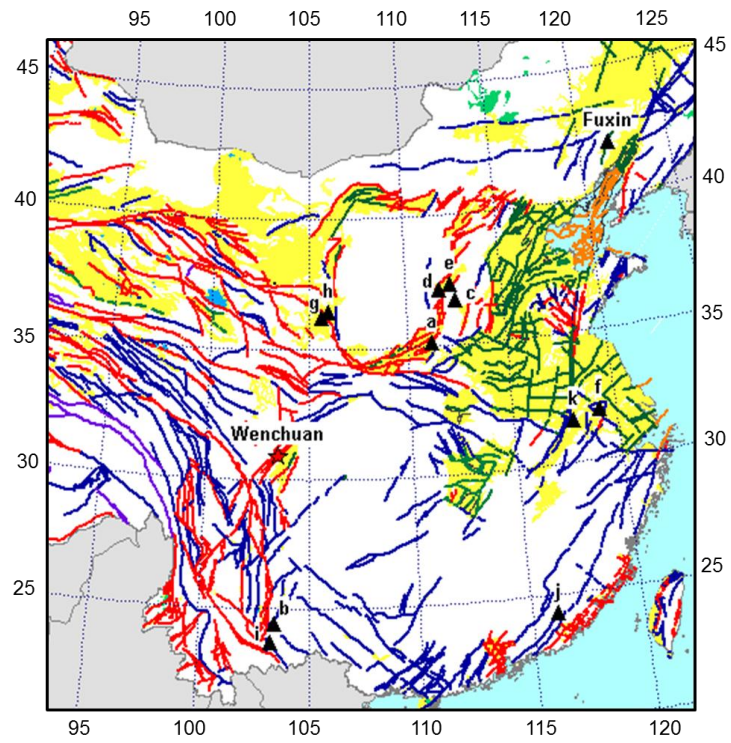


**Figure 1.** The selected 12 stations with distinct amplitude co-seismic water level changes during the Wenchuan earthquake in mainland China. The well numbers are in accordance with the numbers listed in [Table 1](#).

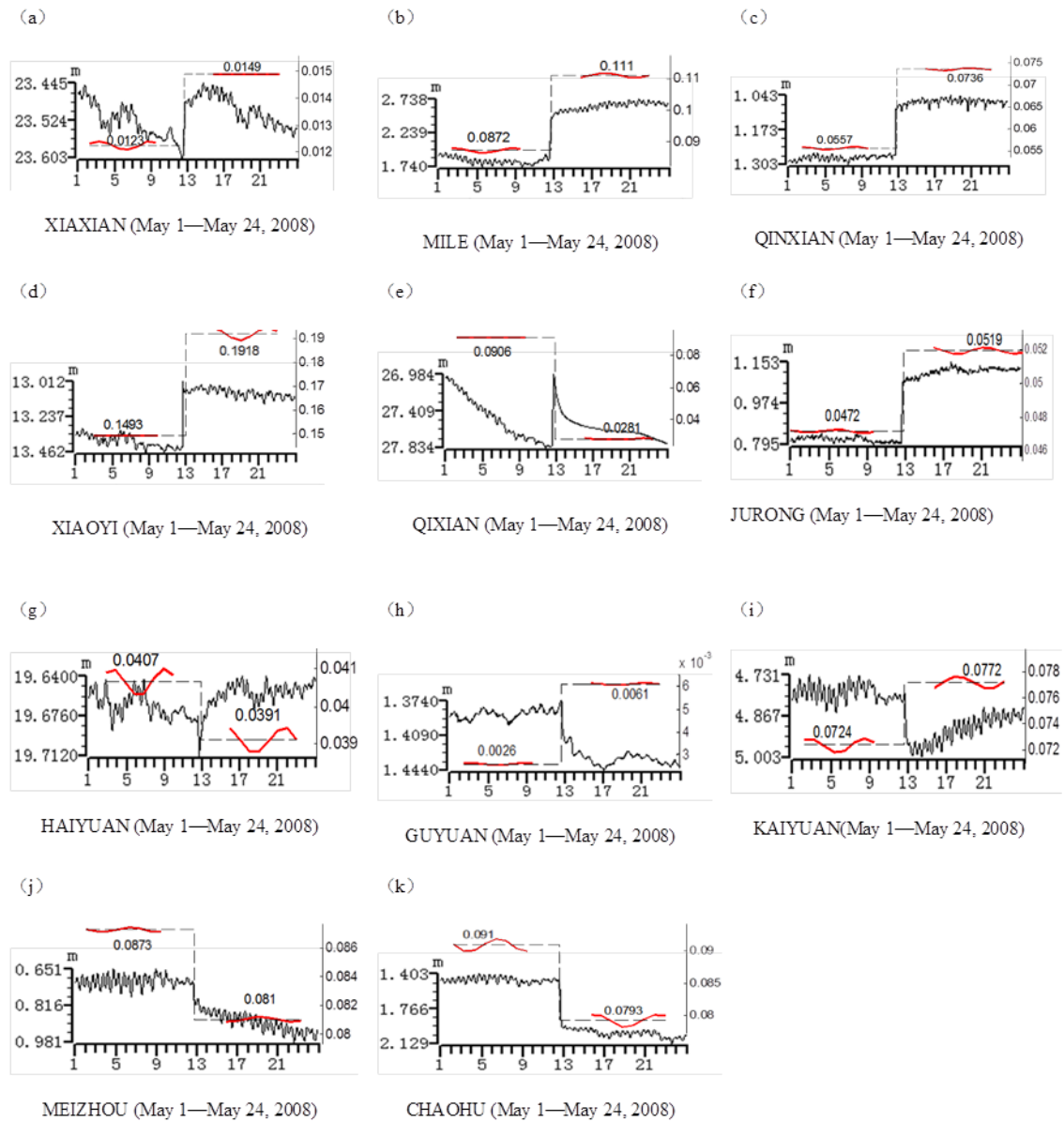


**Figure 2.** (a) Left y-coordinate: original water levels, the sequential number of y-coordinate depends on the type of the well, “sequential number increase from low to high” indicates an artesian well, the coordinate value means the height from the free water surface to the artesian discharge point or to the ground. “Sequential number decrease from low to high” indicates a non-artesian well, and the coordinate value means the depth from the free water surface to the ground. All the ascendant/descendent patterns in the picture indicate water level ascending/ descending. (b) Right y-coordinate: the calculated Skempton’s coefficient  $B$ . The dashed lines

indicate the mean  $B$  values, which are clearly shown in numbers. While the curves along the dashed lines indicate the continuous  $B$  values both pre- and post-earthquake.

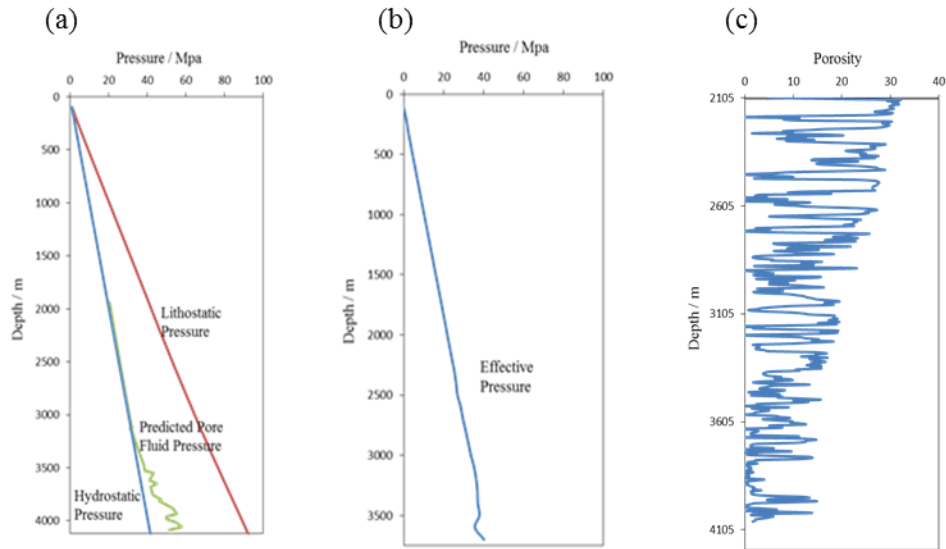


**Figure 3.** (a) Pressure section of W-1 well in Yanchang basin, the bedrock of W-1 well is sandstone. (b) Effective pressure section of W-1 well, we just show the depth above 3500m, so as to see the value in shallow depth more clearly. (c) Porosity section of W-1 well. The porosity records approximately starts from 2100 m, there are no records above this depth.

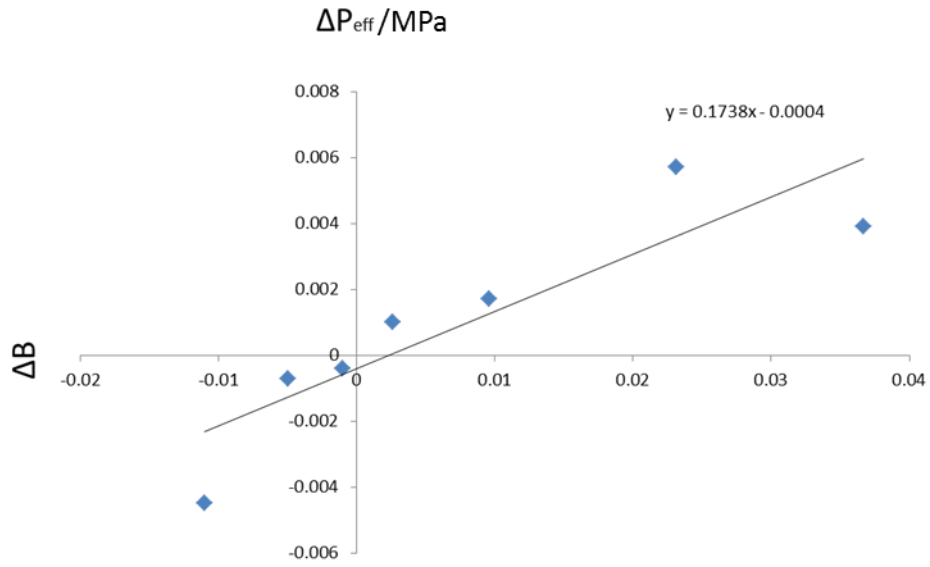
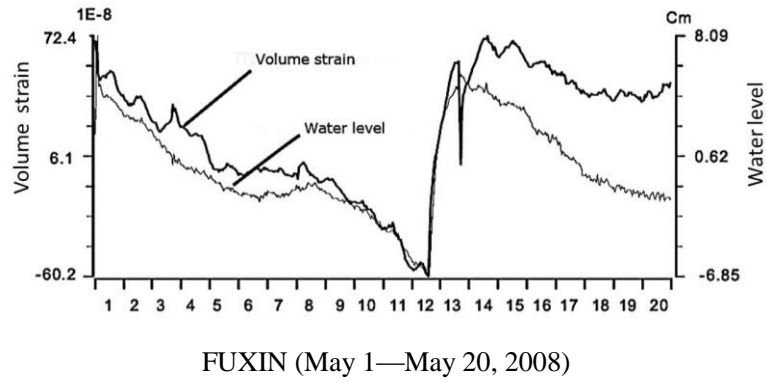


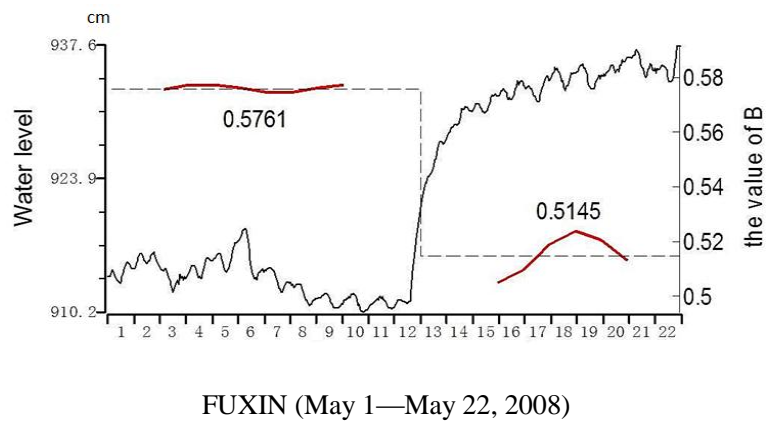
**Figure 4.** The relationship between the change of Skempton's coefficient  $B$  and the change of effective pressure  $P_{\text{eff}}$  of those wells of which the coseismic water level changes can be explained by the consolidation or dilatation caused by teleseismic waves.

(a)





(b)



(c)

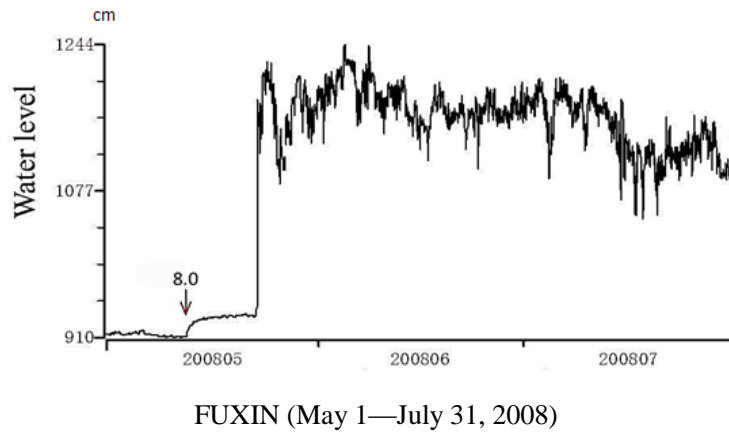
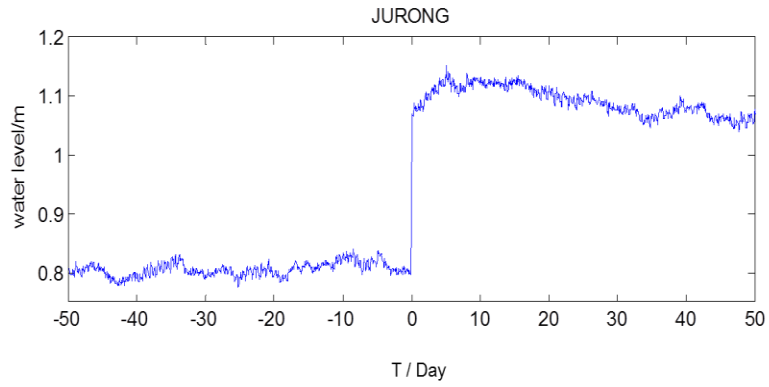


**Figure 5. Fuxin well** (a) Corrected water level and volume strain after removing the influence of atmospheric pressure and tidal strain (based on the harmonic analysis method). In order to avoid the interfere of thunder, there is a power cut protection on 13 May, which is in accordance with the break point of the volume strain in the figure

(Huang, 2008). (b) Original water level and the pre- and post- earthquak Skempton's coefficient  $B$ . (c) Original water level of Fuxin well form May, 2008 to July 2008.

(a)



(b)

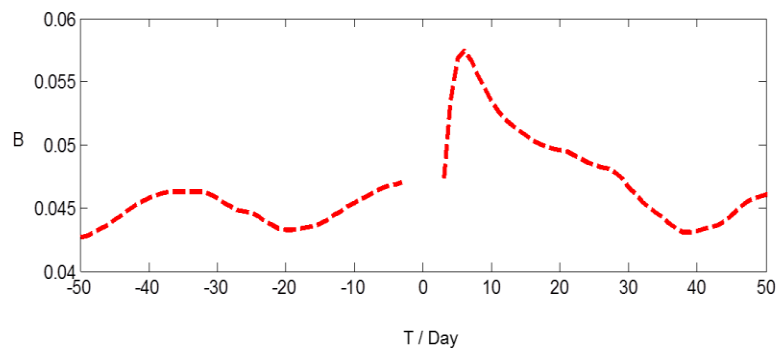


**Figure 6. Jurong well** (a) Original water level of Jurong station. (b) Continuous  $B$  value of Jurong station. (“0” depends the day when Wenchuan earthquake happened)

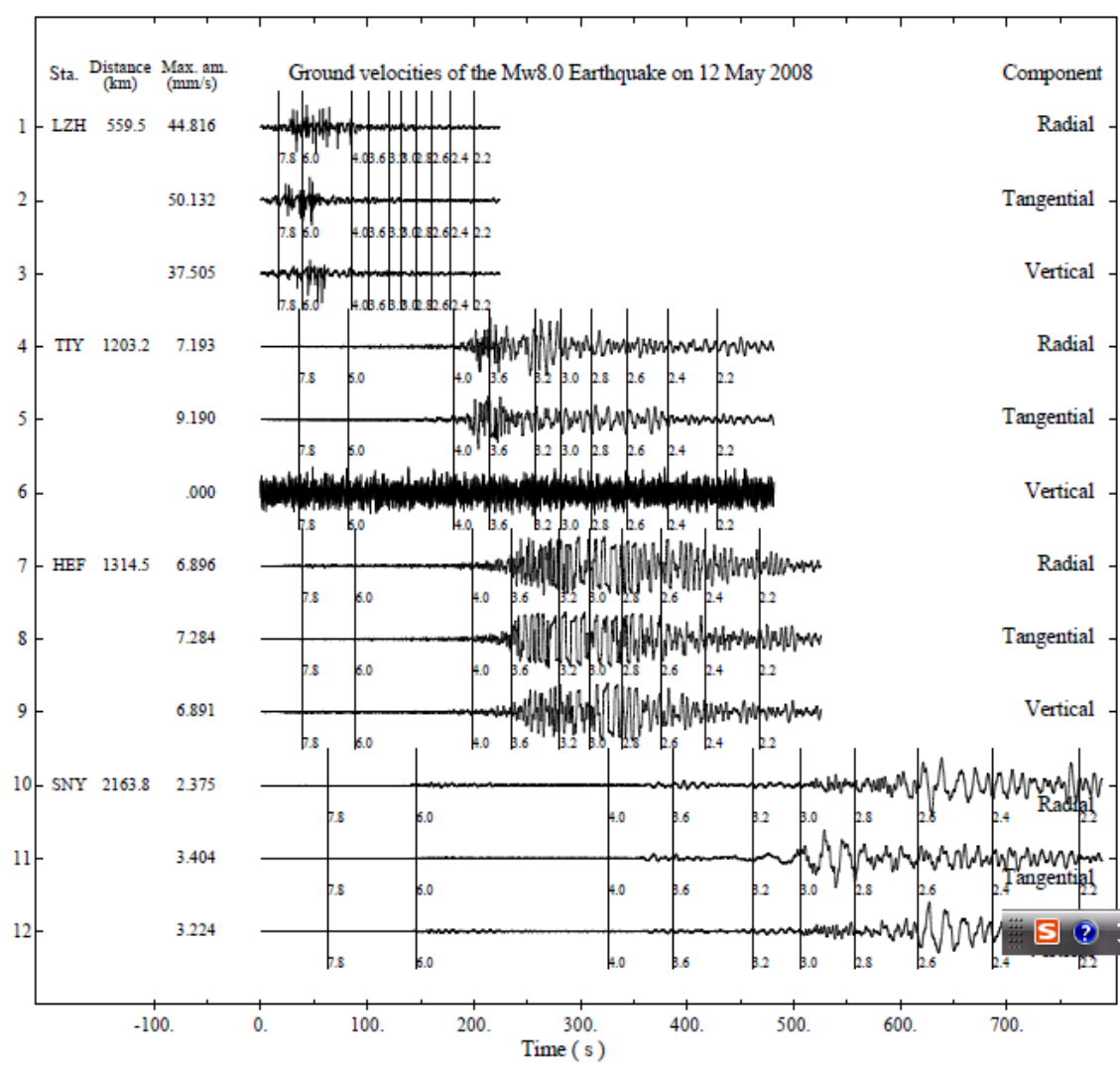
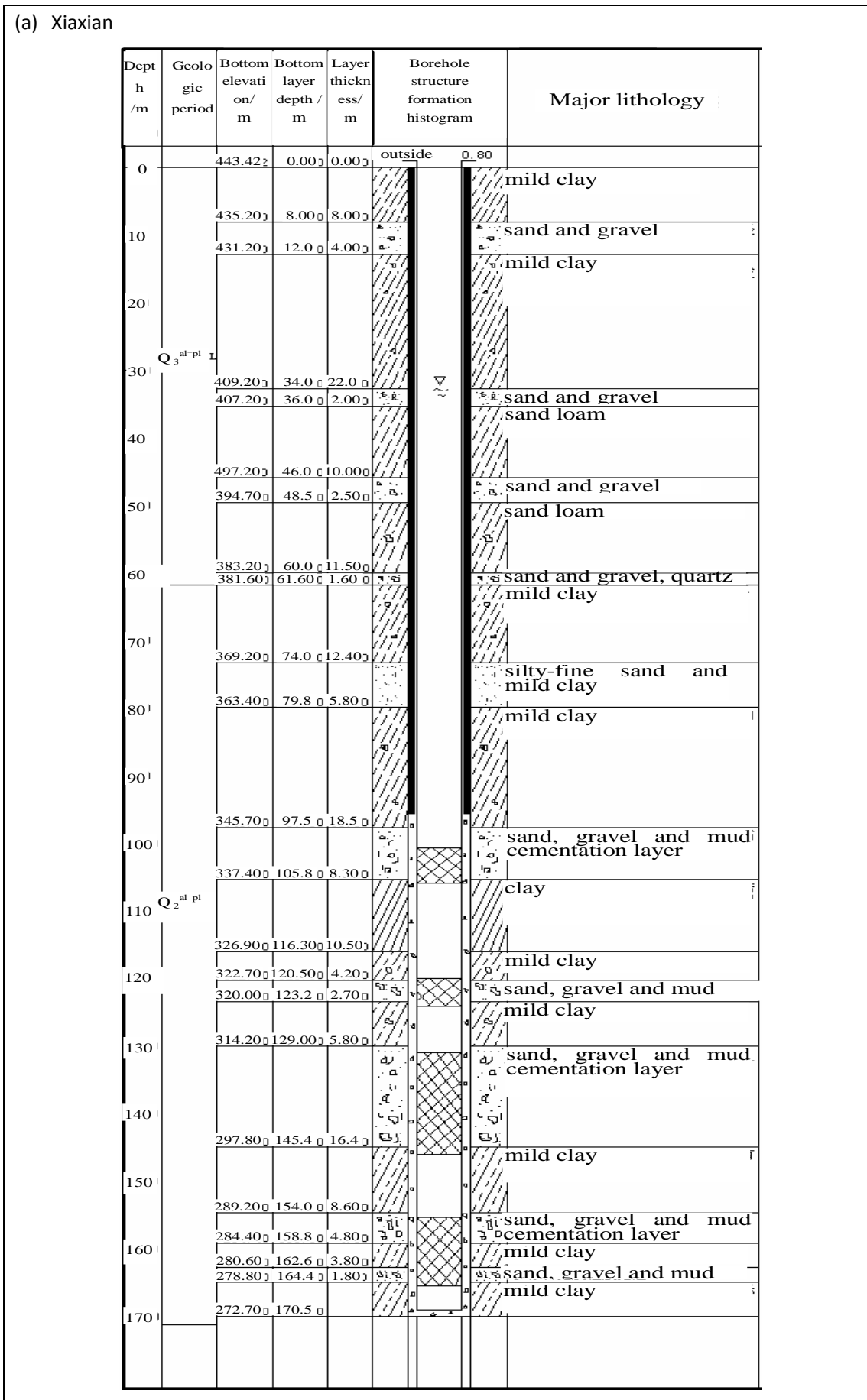
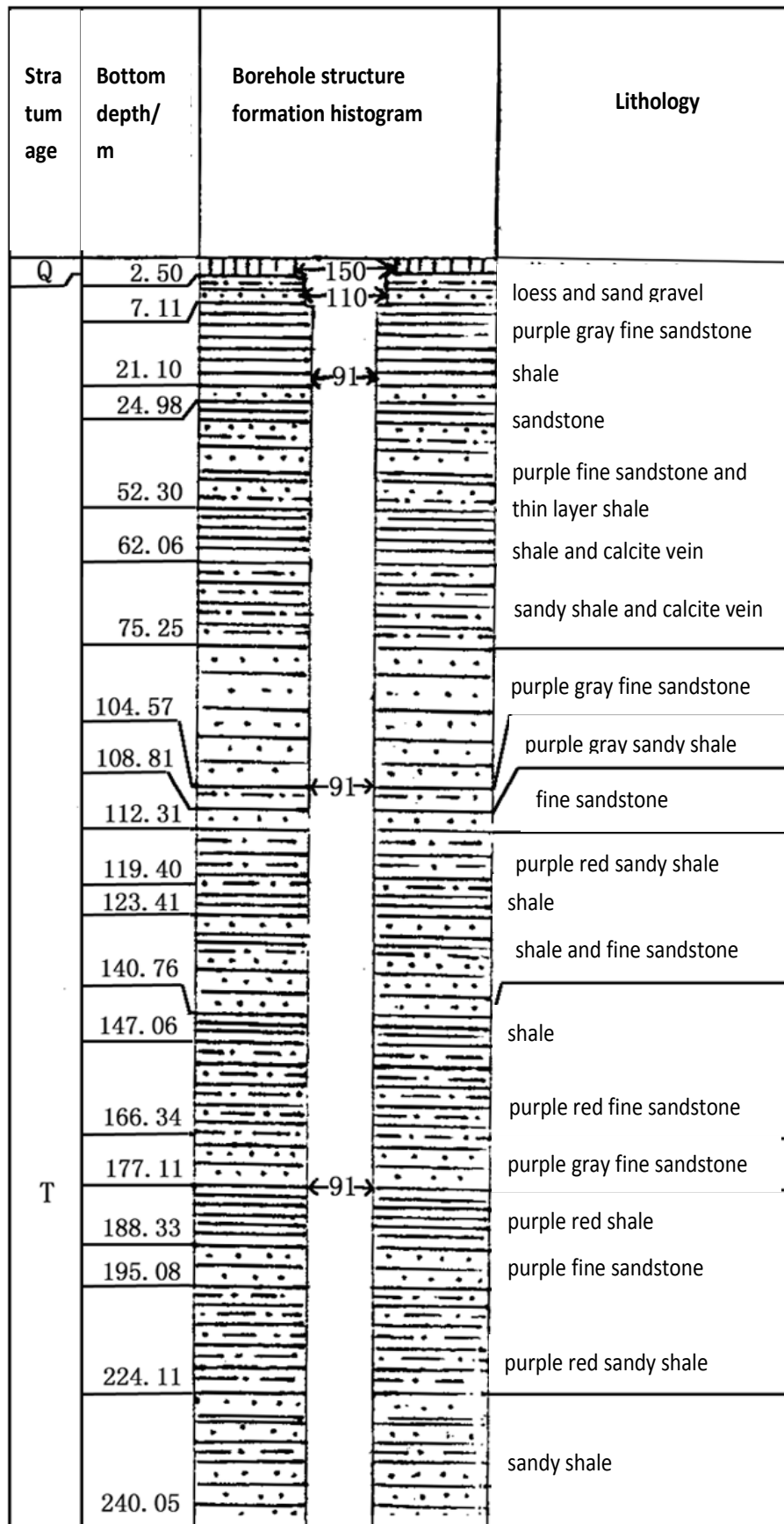


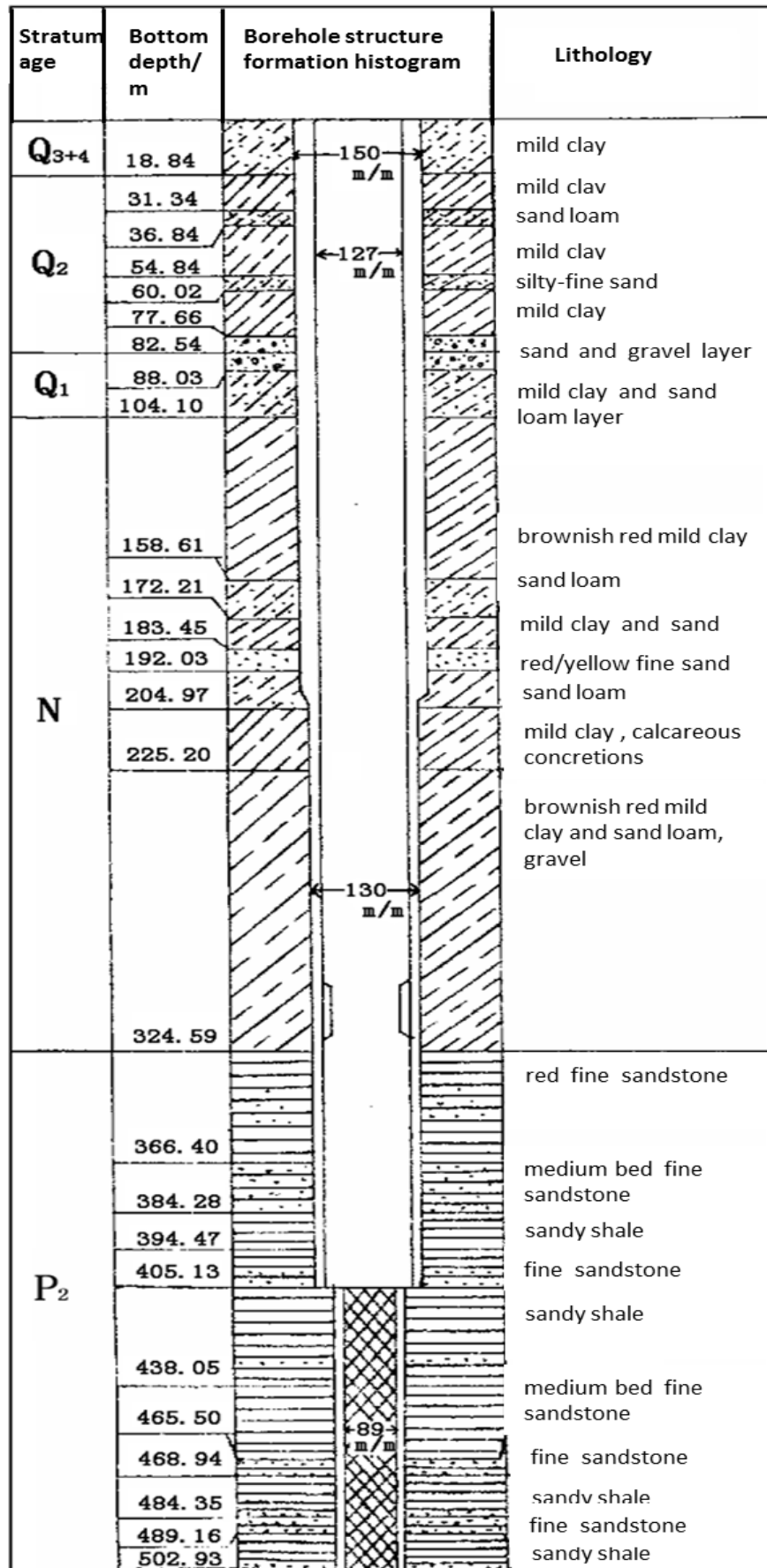
**Figure 7.** Seismograms of the selected 4 national stations for the  $M_s$  8.0 Wenchuan earthquake. The stations are ordered according to their epicentral distances. The station names and maximum amplitudes are listed on the left-hand side and are measured in millimetres per second. Marks (vertical lines) on the waveforms indicate apparent group velocities. “0” is the time of Wenchuan earthquake: at 14:27:59.5, May12, 2008 (Chinese time). (This plotting pattern of seismograms are coined by [Zhao et al.\(2008\)](#)).



(c) Qinxianmanshui



(d) Xiaoyi



(e) Qixian

Stratum	Bottom depth/m	Borehole structure formation histogram	Lithology
Quaternary period	253.79	146m	Loess layer
Tertiary	254.79		Gravel
Triassic	291.65	130m	Limestone and tuff
	349.33		
	442.19		

(f) Jurong

Bottom layer depth (m)	Borehole structure formation histogram	Lithology
0-22.5	Φ 0.38m	clay, silty-fine sand, gravel
22.5-420.0		Φ 0.219m
420.0-500.4	Φ 0.168m	sandstone, argose, rock fragments, gravel interlayer
500.43-696.48		Φ 0.146m
696.48-889.18	Φ 0.127m	



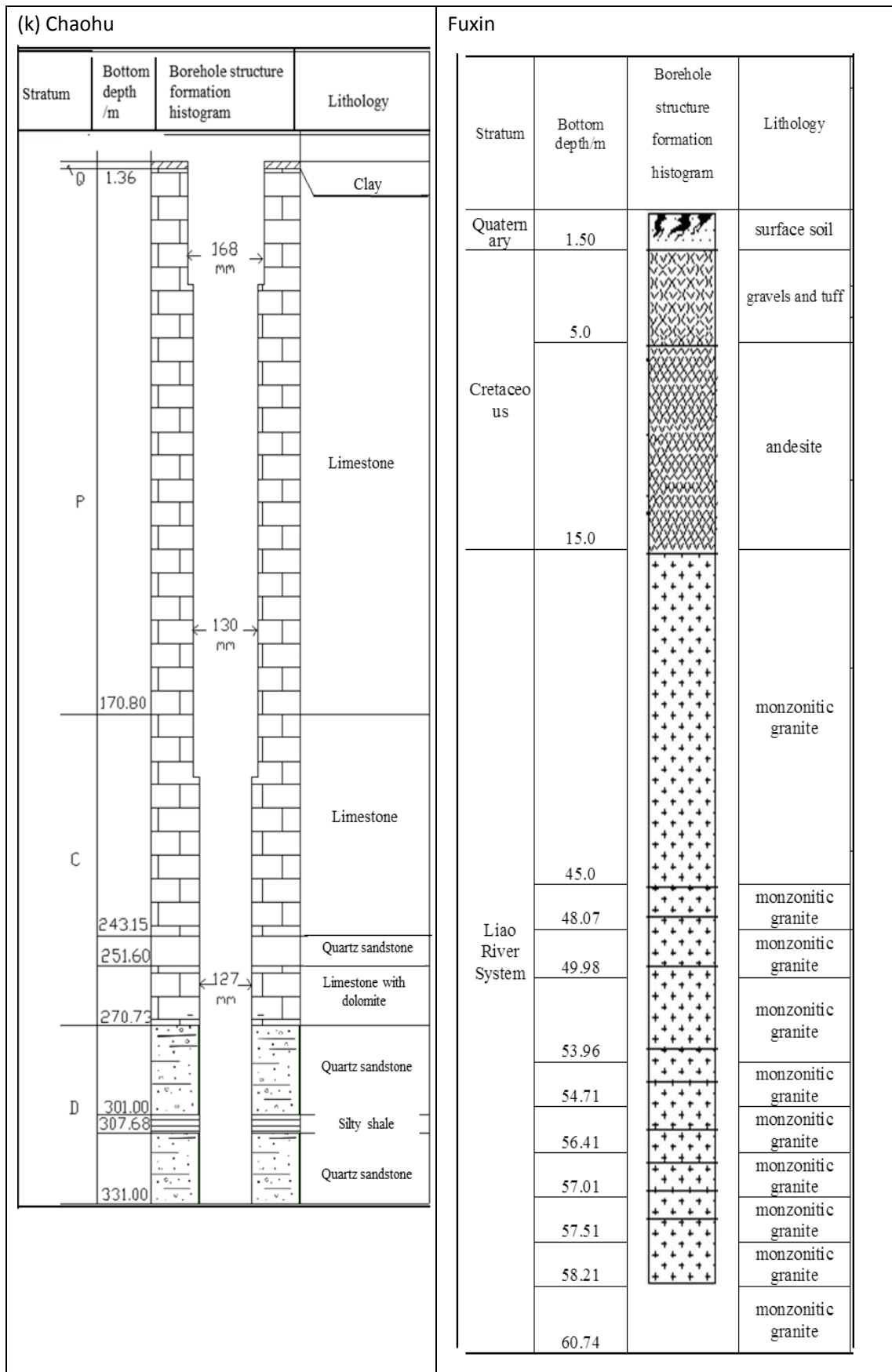


**Figure 7.** Borehole structure formation histogram of well (a), (c), (d), (e), (f), (k) and Fuxin.

*Bulletin of the Seismological Society of America*

COPYRIGHT/PAGE-CHARGES FORM

PLEASE FILL OUT AND SUBMIT THIS FORM ONLINE WHEN SUBMITTING YOUR PAPER  
OR FAX IT TO FAX NUMBER 503 405 7190

Manuscript Number: BSSA-D-\_\_\_\_\_ [leave blank for new submissions]

Title: Studies of mechanism for water level changes induced by teleseismic waves.

Authors: Yan Zhang, Li-Yun Fu, Fugiong Huang and Yichuan Ma.

**COPYRIGHT**

In accordance with Public Law 94-533, copyright to the article listed above is hereby transferred to the Seismological Society of America (for U.S. Government employees, to the extent transferable) effective if and when the article is accepted for publication in the *Bulletin of the Seismological Society of America*. The authors reserve the right to use all or part of the article in future works of their own. In addition, the authors affirm that the article has not been copyrighted and that it is not being submitted for publication elsewhere.

To be signed by at least one of the authors (who agrees to inform the others, if any) or, in the case of "work made for hire," by the employer.



Authorized Signature for Copyright

Yan Zhang

Print Name (and title, if not author)

Dec. 12th, 2012

Date

**PUBLICATION CHARGES**

The Seismological Society of America requests that institutions supporting research share in the cost of publicizing the results of that research. The Editor has the discretion of waiving page charges for authors who do not have institutional support. Current rates are available at <http://www.seismosoc.org/publications/bssa/authors/bssa-page-charges.php>

**Color options:** Color figures can be published in (1) color both in the online journal and in the printed journal, or (2) color online and gray scale in print. Online color is free; authors will be charged for color in print. You must choose one option for all of the color figures within a paper; that is, you cannot choose option (1) for one color figure and option (2) for another color figure. You cannot submit two versions of the same figure, one for color and one for gray scale. You are responsible for ensuring that color figures are understandable when converted to gray scale, and that text references and captions are appropriate for both online and print versions.

**Color figures must be submitted before the paper is accepted for publication. If color figures are changed to gray scale after acceptance of the paper, there will be a delay to publication while the paper undergoes further review by the Editorial Board.**

Art guidelines are at <http://www.seismosoc.org/publications/bssa/authors/bssa-art-submissions.php>

Will page charges be paid? Check one:

**BOTH PAGE CHARGES AND COLOR CHARGES WILL BE PAID**, and all color figures for this paper will be color both online and in print. This option requires full payment of page and color charges. *Before choosing this option, please ensure that there is funding to support color in print.* See <http://www.seismosoc.org/publications/bssa/authors/bssa-page-charges.php> for current rates.

**ONLY PAGE CHARGES WILL BE PAID**, and all figures for this paper will be gray scale in print. Color figures, if any, will be color online.

**A WAIVER OF PAGE CHARGES IS REQUESTED**, and all figures will be gray scale in print. Color figures, if any, will be color online.

Send Invoice To: \_\_\_\_\_  
\_\_\_\_\_  
\_\_\_\_\_

If your paper is accepted for publication, SSA requires that you fill out and submit an online billing/offprint form.

Questions regarding billing should be directed to the SSA Business Office,  
Suite 201, Plaza Professional Building, El Cerrito, CA 94530 USA Phone 510 525-5474 Fax 510 525-7204